ISSN 1016-6254

Österreichische Beiträge zu Meteorologie und Geophysik

Heft 37

The operational Limited Area Modelling system at ZAMG: ALADIN-AUSTRIA

Yong Wang, Thomas Haiden and Alexander Kann

Wien 2006

Österreichische Beiträge zu
Meteorologie und Geophysik

Heft 37

The operational Limited Area Modelling system at ZAMG: ALADIN-AUSTRIA

Wien 2006

Zentralanstalt für Meteorologie und Geodynamik, Wien

Publ.Nr. 418

ISSN 1016-6254

IMPRESSUM

Herausgeber: Zentralanstalt für Meteorologie und Geodynamik (ZAMG), Wien

Leitende Redakteure: Sophie Debit, Fritz Neuwirth, ZAMG, Wien

für den Inhalt verantwortlich:
Yong Wang, Thomas Haiden, Alexander Kann

Druck: Grafisches Zentrum HTU GmbH
1040 Wien, Wiedener Hauptstraße 8-10
www.grafischeszentrum.at

Verlag: Zentralanstalt für Meteorologie und Geodynamik
Hohe Warte 38, A-1190 Wien
Austria (Österreich)

The operational Limited Area Modelling system at ZAMG: ALADIN-AUSTRIA

Yong Wang, Thomas Haiden and Alexander Kann

NWP Division, ZAMG
Hohe Warte 38, A-1190 Wien

CONTENTS

ZUSAMMENFASSUNG

Das NWP Modell ALADIN (**A**ire **L**imitée **A**daptation dynamique **D**éveloppement **I**nter**N**ational) wurde im Rahmen eines internationalen Projektes von 13 Europäischen nationalen Wetterdiensten initiiert und im Jahre 1998 an der ZAMG in den operationellen Betrieb eingeführt. Ein neues operationelles LAM System, ALADIN-AUSTRIA, wurde im Jahre 2003 ins Leben gerufen. Im Zuge dessen wurde nicht nur die horizontale Auflösung erhöht, sondern auch die vertikale von 37 auf 45 Schichten erweitert. Seit Mai 2004 wird dieses Modell im operationellen Dienst verwendet. Der Artikel gibt einen kurzen Überblick über die wichtigsten Modellcharakteristika wie Modellgleichungen, horizontale bzw. vertikale Gitterstruktur, Initialisierung, Kopplung und physikalische Parametrisierungen. Ferner wird die Modellgüte von ALADIN-AUSTRIA beschrieben sowie ein Vergleich zwischen ALADIN-AUSTRIA und seinen Vorgängermodellen ALADIN-LACE und ALADIN-VIENNA gegeben. Dabei zeigt sich, dass besonders im Kurzfristbereich eine leichte Verbesserung der Bodenparameter wie der 2m Temperatur erreicht wird.

ABSTRACT

The limited area numerical weather prediction model ALADIN (**A**ire **L**imitée **A**daptation dynamique **D**éveloppement **I**nter**N**ational) developed by 13 European national weather services within an international project, has been in use operationally at ZAMG since September 1998. A new operational NWP-LAM system, ALADIN-AUSTRIA, was designed in 2003/2004, in which not only the horizontal resolution of the model was increased but also the number of levels from 37 to 45. In May 2004 ALADIN-AUSTRIA was put into operation at ZAMG. The paper gives a brief overview of the main features of ALADIN-AUSTRIA, including model equations, horizontal/vertical representations, initialisations, coupling and physics parameterizations. Furthermore, the performance of ALADIN-AUSTRIA and comparisons between ALADIN-AUSTRIA and ALADIN-LACE/ALADIN-VIENNA, the earlier versions of ALADIN at ZAMG, are discussed. Verification statistics show that ALADIN-AUSTRIA gives a slight improvement for surface parameters like 2m temperature.

1. Introduction

Limited area numerical weather prediction (NWP) models have become the main tool for regional and local weather prediction and research. They are also widely used for providing meteorological input data for applications in hydrology, environmental protection, energy industry, agriculture and transportation. At the beginning of the year 1990 ZAMG faced the necessity of operating a modern Limited Area Model (LAM), and through RC/LACE, Regional Cooperation for Limited Area modelling in Central Europe, ZAMG joined an international project in the field of NWP. Within this international cooperation, ZAMG, together with the 12 other European national weather services (France, Belgium, Portugal, Hungary, Czech, Slovakia, Slovenia, Croatia, Bulgaria, Moldova, Romania, Poland), Morocco and Tunisia, developed the high resolution LAM ALADIN. The growth in computing power at ZAMG made it possible to run a LAM operationally. The first operational LAM at ZAMG, ALADIN-VIENNA, started on 22 September 1998, which was run on a Workstation (DEC Alpha600, 1GB RAM, 600MHZ) twice per day at 00UTC and 12UTC up to 48 hours. It covered Austria and surrounding neighbouring countries (Fig. 1, left) with a horizontal resolution of 9.6km and 31 levels in the vertical. ALADIN-VIENNA was nested in ALADIN-LACE which was run at CHMI in Prague. ALADIN-LACE covers the whole Central Europe (Fig. 1, right) with 12.2km horizontal resolution, and is coupled with the global model ARPEGE/IFS at Meteo-France (Action de Recherche Petiet Echelle Grande Echelle / Integrated Forecasting System, Courtier and Geleyn, 1988). At that time the operational model chain consisted of three steps.

ARPEGE (Toulouse) ---> ALADIN-LACE (Prague) ---> ALADIN-VIENNA (Vienna).

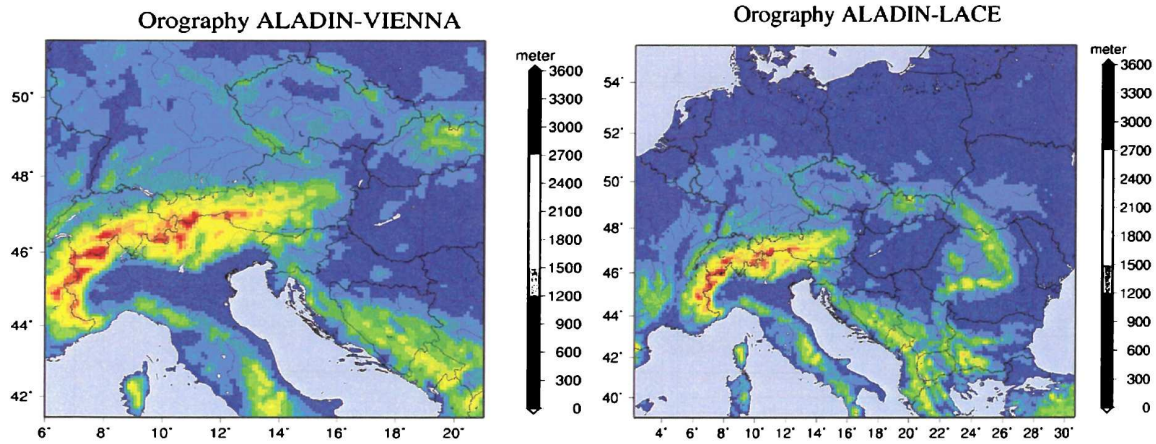

Figure 1: The model domain and topography of ALADIN-VIENNA (left) and ALADIN-LACE (right).

In January 2002, a high performance computer SGI-3400 became available through project *„Krisenrechnung* " at ZAMG. Starting on 4th of February 2002, ALADIN-VIENNA was run operationally on SGI, and ALADIN-LACE was also run routinely at ZAMG since 1 January 2003. The operational procedure was replaced by

ARPEGE (Toulouse) ---> ALADIN-LACE (Vienna) ---> ALADIN-VIENNA (Vienna).

The models ALADIN-VIENNA and ALADIN-LACE differed merely in the horizontal resolution and the size of the domain, whereas the vertical resolution was 37 levels for both.

Recently, different LAM models have been used for weather prediction and research at very high horizontal resolution. Indeed, the example of Meso-NH (Lafore et al., 1998) has shown that very high horizontal resolution (2-3km) with better model physics can improve the quality of the numerical forecast. However, one may question the adequacy of vertical resolution in the current NWP models. Experience at ZAMG with ALADIN-VIENNA and ALADIN-LACE shows that increasing the horizontal resolution alone cannot guarantee a better forecast.

Lindzen and Fox-Rabinovitz (1989) derived a consistency criterion between horizontal resolution ΔX and vertical resolution ΔZ, for example, for quasi-geostrophic flows,

$$\Delta Z = \frac{f}{N} \Delta X \qquad (1)$$

where f is the Coriolis parameter and N is the buoyancy frequency. It is apparent from Eq. (1), that vertical and horizontal resolution should be proportional to each other. Pecnick and Keyser (1989) studied the relationship between ΔZ and ΔX for a frontal structure, Persson and Warner (1991) for the conditional symmetric instability associated with frontal systems. Similar investigations were also conducted to examine the importance of model resolution consistency in heat transport (Weaver and Sarachik, 1990), and cloud and radiation parameterizations (Lane et al. 2000). All these studies suggested that one should not simply increase the horizontal resolution without considering appropriate vertical resolution. In addition, they indicated that a consistent model resolution would lead to more realistic simulations and eliminate some artificial features and noise, such as spurious gravity waves.

In order to improve forecast quality, to use computer power more efficiently, and to simplify the operational production procedure of the NWP system at ZAMG, a new project was started at the end of 2003. The result was a new NWP-LAM system ALADIN-AUSTRIA with the following main features:

- The vertical resolution is increased from 37 to 45, the most additional levels are located in the lower atmosphere. A schematic comparison of the vertical levels between ALADIN-AUSTRIA and ALADIN-LACE/ALADIN-VIENNA is shown in Fig. 2.

- The model domain is almost the same as ALADIN-LACE, see Fig. 3.

- The horizontal resolution is set to 9.6km, similar to ALADIN-VIENNA.

Thus, the operational procedure of NWP-LAM system at ZAMG became simply:

ARPEGE (Toulouse) ---> ALADIN-AUSTRIA (Vienna) .

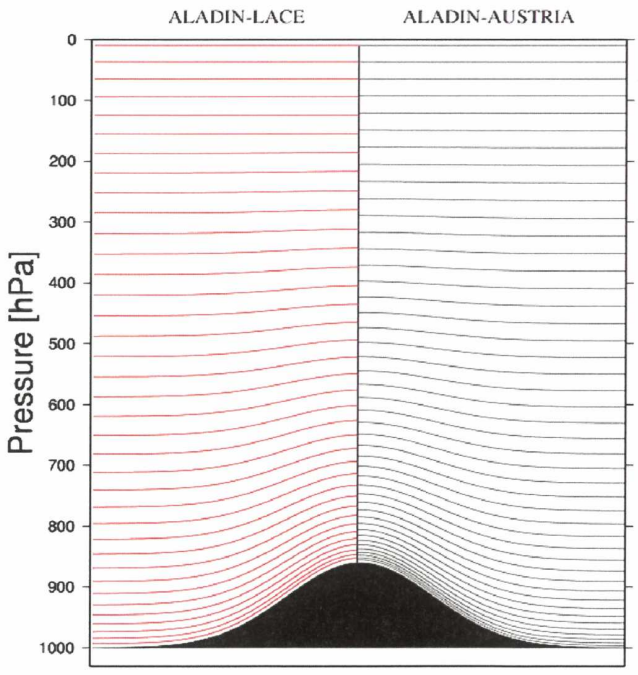

Figure 2: Comparison of vertical levels in ALADIN-LACE/ALADIN-VIENNA and ALADIN-AUSTRIA. Most of the additional levels are located in the lower atmosphere.

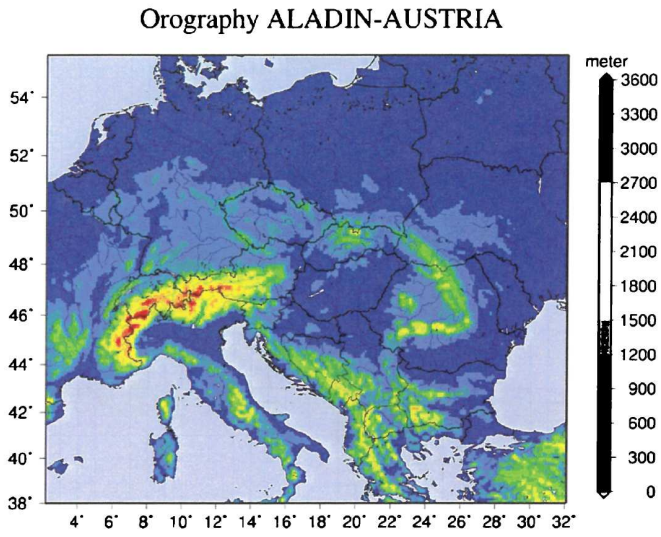

Figure 3: Domain and model topography of ALADIN-AUSTRIA.

ALADIN-AUSTRIA replaced both ALADIN-VIENNA und ALADIN-LACE. In this way the maintenance work of the operational system was reduced while at the same time the quality of the forecast was kept or slightly increased. After a 2-month parallel test with ALADIN-LACE and ALADIN-VIENNA, ALADIN-AUSTRIA was put into operations on 10 May 2004.

In this paper, ALADIN-AUSTRIA is described in Section 2. Model equations, horizontal and vertical representation, coupling, initialisation, time integration scheme, and physics parameterisation are presented. The verification of results of ALADIN-AUSTRIA, ALADIN-LACE and ALADIN-VIENNA against analysis and observations is discussed in Section 3. The concluding Section contains a summary and outlook to future work.

2. The model dynamics and physics in ALADIN-AUSTRIA

ALADIN-AUSTRIA is a hydrostatic, spectral limited area model, which is coupled with its global counterpart ARPEGE. This section presents briefly the model equations, horizontal and vertical representation, initialisation, coupling, time integration, horizontal diffusion and physics parameterisations.

2.1 The Model Equations

2.1.1 Vertical Coordinate

The vertical coordinate of the model is the pressure-based hybrid coordinate η proposed by Simmons and Burridge (1981)

$$P(x,y,\eta,t) = A(\eta) + B(\eta)\pi(x,y,t)\,, \tag{2}$$

where η is the vertical coordinate, p is pressure, π is the surface pressure and A and B are constants depending on the vertical levels. The coordinate η varies between 0 (at the top) and 1 (at the bottom) and the following conditions are fulfilled

$$A(1) = 0; \qquad B(1) = 1; \qquad B(0) = 0; \qquad \frac{\partial \eta}{\partial p} > 0.$$
$$\lim_{\eta \to 1} p = \pi(x,y,t); \qquad \lim_{\eta \to 0} p = p_{top} = const. \tag{3}$$

Therefore η is defined by the constants A and B. This coordinate is terrain following at low levels, and becomes a pure pressure coordinate at upper levels.

2.1.2 Momentum Equations

The equations of motion for ALADIN-AUSTRIA in the physical space are

$$\frac{\partial v}{\partial t} = -u[\partial_x v] - v[\partial_x u] + Dv - \left(\dot{\eta}\frac{\partial p}{\partial \eta}\right)\frac{\partial v}{\partial p} + KC_{bv}(\varphi,\lambda) + fu - (RT\partial_y \ln p + \partial_y \phi) - g\left(\frac{\partial p}{\partial \eta}\right)\frac{\partial F_v}{\partial p} + m(\partial_t v')^{diff.h.} \quad (4)$$

$$\frac{\partial u}{\partial t} = -u[\partial_x u] - v[\partial_x v] + \zeta v - \left(\dot{\eta}\frac{\partial p}{\partial \eta}\right)\frac{\partial u}{\partial p} + KC_{bu}(\varphi,\lambda) + fv - (RT\partial_x \ln p + \partial_x \phi) - g\left(\frac{\partial p}{\partial \eta}\right)\frac{\partial F_u}{\partial p} + m(\partial_t u')^{diff.h.} \quad (5)$$

where u and v are the physical wind components projected on the frame of the ALADIN grid, u' and v' are the wind components on the map, R is the gas constant, T is the temperature, f the Coriolis parameter, ϕ is the geopotential, ζ and D are the vorticity and divergence, $K = \frac{(u^2+v^2)}{2}$ is the kinetic energy, F_u and F_v represent the physical forcing, which are vertical turbulent diffusion, vertical exchange of momentum due to convection, vertical transport of momentum due to unresolved gravity waves generated by the small scale changes of the orography, and the tendency resulting from momentum transport by falling precipitation. The last terms $(\partial_t u')^{diff.h.}$ and $(\partial_t v')^{diff.h.}$ represent the effect of turbulent horizontal diffusion. $\left(\dot{\eta}\frac{\partial p}{\partial \eta}\right)$ denotes the advecting vertical velocity.

m represents the map scale factor for either the Polar Stereographic, Lambert Comformal or Meractor map projections. In ALADIN-AUSTRIA the Lambert Conformal projection is used, then m reads:

$$m = \left(\frac{\cos\varphi_0}{\cos\varphi}\right)^{1-K_L}\left[\frac{1+\sin\varphi_0}{1+\sin\varphi}\right]^{K_L} \quad (6)$$

λ, φ are the longitude and latitude respectively, λ_0, φ_0 are reference longitude and latitude, K_L is a constant parameter. The definitions of geographical coordinates in ALADIN-AUSTRIA are as follows:

$\lambda_0 = 17.0, \varphi_0 = 46.2447$, $K_L = 0.7223$, *not rotated*

The curvature terms in Eq. (4) and (5) C_{bu} and C_{bv} are defined by:

$$C_{bu} = \frac{\sin\varphi - K_L}{a\cos\varphi}\sin K_L(\lambda - \lambda_0) \tag{7}$$

$$C_{bv} = \frac{\sin\varphi - K_L}{a\cos\varphi}\cos K_L(\lambda - \lambda_0) \tag{8}$$

where a is the radius of the earth.

The relationship between the physical wind u, v and the wind on map u', v' after Courtier and Geleyn (1988) is defined as

$$u = mu', \qquad v = mv' \tag{9}$$

The physical components of gradients of all scalar variables (e.g. for π) then can be written as

$$\partial_x \pi = m\partial'_x \pi, \qquad \partial_y \pi = m\partial'_y \pi \tag{10}$$

In case of the wind vector, the pseudo-physical gradient tensor introduced in Eqs. (4) and (5) will be denoted as

$$[\partial_x u] = m^2 \partial'_x u', \qquad [\partial_x v] = m^2 \partial'_x v' \tag{11}$$

The actual physical wind gradient tensor components are

$$\partial_x u = m\,\partial'_x (m(x,y)u') \neq m^2 \partial'_x u'. \tag{12}$$

2.1.3 Hydrostatic and Continuity Equations

The essential diagnostic equation in ALADIN-AUSTRIA dynamics is the hydrostatic constraint (Simmons and Burridge, 1981),

$$\frac{\partial\phi}{\partial\eta} = -\frac{RT}{p}\frac{\partial p}{\partial\eta} \tag{13}$$

The continuity equation, expressing mass conservation, is written as

$$\frac{\partial}{\partial t}\left(\frac{\partial p}{\partial\eta}\right) = -\nabla\cdot\left(V\frac{\partial p}{\partial\eta}\right) - \frac{\partial}{\partial\eta}\left(\dot{\eta}\frac{\partial p}{\partial\eta}\right), \tag{14}$$

with

$$\nabla\cdot\left(V\frac{\partial p}{\partial\eta}\right) = \left(\frac{\partial p}{\partial\eta}\right)D + \frac{dB}{d\eta}(u\partial_x\pi + v\partial_y\pi). \tag{15}$$

The vertical integral of Eq. (14) is used to compute the temporal variation of the surface pressure π in the model,

$$\frac{\partial \pi}{\partial t} = -\int_0^1 \nabla \cdot \left(V \frac{\partial p}{\partial \eta} \right) d\eta \,. \tag{16}$$

Noting that, at any η level,

$$\frac{\partial}{\partial t}\left(\frac{\partial p}{\partial \eta} \right) = \frac{dB}{d\eta} \frac{\partial \pi}{\partial t}, \tag{17}$$

after calculation of the surface pressure tendency $\frac{\partial \pi}{\partial t}$, the advecting vertical velocity is obtained at each level in the model by vertical integration of Eq. (14)

$$\left(\dot{\eta} \frac{\partial p}{\partial \eta} \right) = -B(\eta) \frac{\partial \pi}{\partial t} - \int_0^{\eta} \nabla . \left(V \frac{\partial p}{\partial \eta} \right) d\eta \tag{18}$$

Finally, the pressure vertical velocity can be expressed by

$$\omega = \frac{\partial p}{\partial t} + (V.\nabla) p + \left(\dot{\eta} \frac{\partial p}{\partial \eta} \right) = B(\eta) V \nabla \pi \frac{\partial \pi}{\partial t} - \int_0^{\eta} \nabla . \left(V \frac{\partial p}{\partial \eta} \right) d\eta \,. \tag{19}$$

2.1.4 Thermodynamic and Moisture Equations

The thermodynamic and moisture equations in the model are

$$\frac{\partial T}{\partial t} = -u \partial_x T - v \partial_y T - \left(\dot{\eta} \frac{\partial p}{\partial \eta} \right) \frac{\partial T}{\partial p} + \frac{RT}{C_p} \frac{\omega}{p} - g \left(\frac{\partial p}{\partial \eta} \right) \frac{\partial F_T}{\partial p} + m(\partial_t T)^{diff.h.} \tag{20}$$

$$\frac{\partial q_v}{\partial t} = -u \partial_x q_v - v \partial_y q_v - \left(\dot{\eta} \frac{\partial p}{\partial \eta} \right) \frac{\partial q_v}{\partial p} - g \left(\frac{\partial p}{\partial \eta} \right) \frac{\partial F_{q_v}}{\partial p} + m(\partial_t q_v)^{diff.h.} \tag{21}$$

Where C_p is the specific heat at constant pressure and the variations of C_p and latent heat with temperature are taken into account. q_v denotes the specific humidity. Again, as in the momentum equations (4) and (5), $(\partial_t T)^{diff.h.}$ and $(\partial_t q_v)^{diff.h.}$ represent the effects of horizontal diffusion. The terms containing F_T and F_q represent diabatic heating and moistening, which include several physical processes, e.g. for temperature

- vertical turbulent diffusion, including the turbulent re-distribution of heating at the surface,
- vertical fluxes due to convection,
- heating/cooling due to condensation of rain in stratified or convective clouds, evaporation of rain, basically conversions between all three water phases
- flux divergences due to short- and longwave radiative fluxes,

For moisture, there are counterparts of the first three processes mentioned above.

2.2 Horizontal representation

It was decided at the beginning of the ALADIN international cooperation that the model should be developed as the LAM counterpart of the global spectral model ARPEGE/IFS in order to share the development and progress in ARPEGE and to use the existing source code of ARPEGE as much as possible. Consequently, ALADIN is formulated in the spectral way with regard to horizontal discretization. A method more frequently used for LAMs is the traditional grid point method. The spectral method has many useful features and advantages compared to the grid-point method, but of course it also has disadvantages which have been often disputed in the NWP world (Geleyn, 1998). We summarize the pros, equals and cons of the spectral method as follows.

The pros:

- ✓ Simple computation of derivatives.
- ✓ No linear phase error in Eulerian mode, no source of non-linear instability, no aliasing error for the computation of quadratic terms.
- ✓ On the sphere, there is no pole problem with the spectral method.
- ✓ The horizontal and vertical components are well separated allowing simplified conservation properties.
- ✓ One can use the simplest A-grid (Arakawa classification) without negative impact, which leads to additional benefits using a semi-Lagrangian technique, as different trajectories (and hence interpolations) for different prognostic quantities can be avoided.
- ✓ More convenient for a semi-implicit time integration scheme, because the Helmholtz equations are trivially solved in a spectral model, this diagonalization property is also useful for variational data assimilation.
- ✓ Implicit horizontal diffusion which is absolutely stable is trivial and infinitely tunable in a spectral model.
- ✓ Spectral fitting, or truncation, is a powerful way to remove numerical noise.
- ✓ Reduced degrees of freedom in spectral space are a favourable feature for various applications in post-processing and in variational calculations.

The equals:

- similar performance on accuracy and computation cost (Gustafsson and McDonald, 1996).

The cons:

- x Steep local gradients may be not well represented in a spectral model, Gibbs phenomenon (Majewski, 1998)
- x Spectral fitting of positive definite quantities (e.g. specific humidity, cloud liquid water and turbulent kinetic energy) can lead to unrealistic results through the Gibbs phenomenon.
- x The model topography is poorly represented in spectral models, there may be unphysical hills and valleys over the oceans after spectral transformation.
- x It is impossible in practice to implement a flow dependent operator for horizontal diffusion in a spectral model (Geleyn, 1998; Weaver and Courtier 2001).
- x The spectral method can not be easily used in the global case for very high truncations (Caian and Geleyn, 1997).

There are still some other arguments against the spectral method as the horizontal resolution becomes higher, for example, the spectral model requires global communication for spectral transforms at each time step; the cost of the Legendre transform increases drastically. But experiences at ECMWF (Temperton, 1998) show that these problems are solvable.

Application of the spectral method on a limited area domain is not as self-evident as in the case of a global one, since periodicity is missing. Machenhauer and Haugen (1987) proposed a way for full harmonic expansion of the grid-point fields for spectral limited area applications and developed the formulation in HIRLAM (Haugen and Machenhauer, 1993). The idea is that the grid-point fields are made bi-periodically by creating an artificial extension zone in which they are interpolated between the values at the opposite edges in both directions. This was implemented in ALADIN.

The horizontal geometry of ALADIN-AUSTRIA is decomposed into three zones as shown in Fig. 4.

- Central zone **C**: the area of meteorological interest.
- Intermediate zone **I**: the area for relaxation or coupling which introduces the forecasts from the large scale model ARPEGE as lateral boundary conditions for ALADIN.
- Extension zone **E**: the artificial area for the application of spectral technique, where the fields are created for having the periodicity conditions in both x and y directions.

The model fields over the areas **C** and **I** are meteorologically and geographically meaningful, the results over the area E are merely used for mathematical operations which are needed by the spectral method.

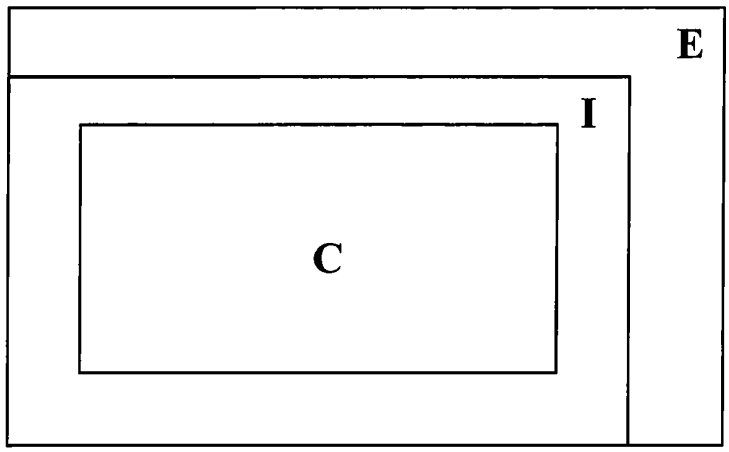

Figure 4: The horizontal geometry of ALADIN-AUSTRIA. The **C**entral zone: the area of meteorological interest; the **I**ntermediate zone: the relaxation area for the coupling; the **E**xtension zone: the area for doubly-periodicisation.

Following the idea by Machenhauer and Haugen (1987) and considering a variable *X*, its full harmonic Fourier expansion is given by

$$X(x,y,\eta,t) = \sum_{m=-M}^{M} \sum_{n=-N}^{N} X_m^n(\eta,t) e^{2i\pi(mx/L_x + ny/L_y)} \tag{22}$$

where M, N are the maximum wave numbers, and L_x, L_y are the horizontal wavelengths in x and y directions respectively. Let J, K be the number of grid-points of the total domain including the **E** zone along the x and y directions respectively. The inverse truncated Fourier transform, i.e. the spectral coefficient X_m^n, is obtained by

$$X_m^n(\eta,t) = \frac{1}{JK} \sum_{j=0}^{J-1} \sum_{k=0}^{K-1} X(j,k,\eta,t) e^{-2i\pi(jm/J + kn/K)} . \tag{23}$$

All transformations, the direct one from the physical space to spectral space and the inverse one from spectral to physical space, are performed in x and then in y direction separately.

Due to the fact that the series are truncated finitely, it is necessary to introduce a constraint in the form of an elliptic spectral truncation, which is illustrated in Fig. 5 and is written for any wave numbers n and m as

$$\frac{n^2}{N^2} + \frac{m^2}{M^2} \leq 1 \tag{24}$$

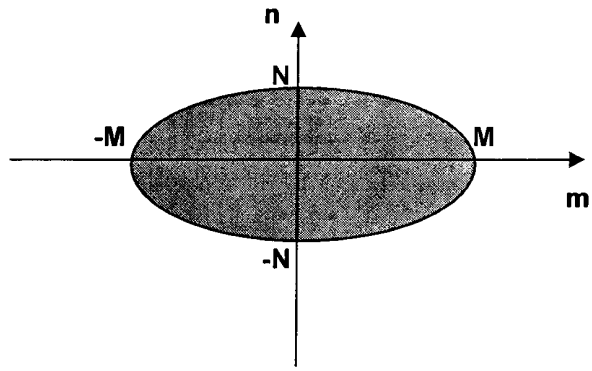

Figure 5: The elliptic truncation of allowed wave numbers in both x and y direction.

This constraint ensures that the spectral representation of the fields over the whole integration domain is isotropic and homogeneous. The elliptic truncation has the same properties on the Cartesian plane as the triangular truncation of the spherical harmonics on the sphere.

The number of modes involved in both Eq. (22) and Eq. (23) in spectral space is $2M + 1$, $2N + 1$, and in physical space J, K grid-points. Those parameters are dependent on each other, because M and N are chosen according to the size of the model domain. If J and K are not well chosen, an aliasing error will be introduced due to the transformations of the quadratic terms in the model equations, which may lead to non-linear instability. To obtain an aliasing-free representation of quadratic terms in the transform grid, the relationship between the numbers of grid-points and the waves in ALADIN should be:

$$J \geq 3M+1 \quad and \quad K \geq 3N+1 \tag{25}$$

However, in the present formulation of ALADIN, the quadratic term also includes map factors (see Eq. (4) and Eq. (5)), for example the momentum advection which creates a fourth-order term. This generates an additional source of aliasing. Specific treatment of this problem as designed for ALADIN is described by Geleyn (1998).

The transforms are carried out by using a Fast Fourier Transform (FFT) technique. Therefore, there are also some other special requirements for J and K.
In ALADIN-AUSTRA we define 8 grid points as the width of the **I** zone, 11 grid points as the width of the **E** zone. The other definitions are

$J = 300$: number of grid-point in x direction for the **C+I+E** domain
$M = 99$: truncation in x direction

$K = 270$: number of grid-point in y direction for the **C+I+E** domain.
$N = 89$: truncation in y direction

The South-West corner of the **C+I** domain: $\lambda_1 = 2.178340150 \quad , \varphi_1 = 33.99584219$
The North-East corner of the **C+I** domain: $\lambda_2 = 39.07586307 \quad , \varphi_2 = 55.64347201$

2.3 Vertical discretisation

As mentioned in section 2.1.1, ALADIN is written in hybrid η coordinates where η is defined by Eq. (2). After Simmons and Burridge (1981) the coordinates provide conservation of energy and angular momentum if the vertical and horizontal discretization schemes are properly chosen.

ALADIN-AUSTIRA is discretized vertically into 45 layers, i.e., 46 η levels, which is illustrated in Table 1. Model variables are staggered in the vertical. Fluxes and the advecting vertical velocity are defined

on full η levels. All other variables are defined on half-η - levels, which are exactly halfway between the full levels. These variables represent layer-mean averages. η is implicit in the coordinate, which means that the fixed layer depths $\delta\eta$ can be eliminated. As a result, all the equations involve only pressure as an explicit vertical coordinate.

Vertical Index K	Constant *A*	Constant *B*	Definition of the Model variables
1	0.0	0.0000000000	$(\dot{\eta}\ \partial p/\partial\eta)=0,\ \eta=0$
2	271.828186	0.0000000019	
3	518.944702	0.0028842613	
4	742.211609	0.0085220076	
5	942.490906	0.0167825148	
6	1120.644653	0.0275349915	
7	1277.534912	0.0406487212	
8	1414.023682	0.0559929237	
9	1530.973022	0.0734368414	
10	1629.244873	0.0928497463	
11	1709.701416	0.1141008511	
12	1773.204468	0.1370594203	
13	1820.616455	0.1615946889	
14	1852.799194	0.1875759512	
15	1870.614624	0.2148723602	
16	1874.924805	0.2433532178	
17	1866.591431	0.2728877664	
18	1846.477783	0.3033452630	
19	1815.444336	0.3345949352	
20	1774.354126	0.3665059805	
21	1724.068604	0.3989477158	
21 1/2			$V,\ T,\ q_v,\ RT\nabla lnp+\nabla\phi,\ \omega$
22	1665.450562	0.4317893684	
23	1599.360596	0.4649002254	
24	1526.662354	0.4981494546	
25	1448.217041	0.5314063430	
26	1364.887939	0.5645400286	
27	1277.534912	0.5974200368	
28	1187.021851	0.6299152970	
29	1094.209106	0.6618951559	
30	999.959656	0.6932288408	
31	905.135925	0.7237858176	
32	810.599121	0.7534350753	
33	717.211487	0.7820459008	
34	625.836548	0.8094877005	
35	537.334961	0.8356295824	
36	452.567444	0.8603407741	
37	372.398499	0.8834904432	
38	297.689941	0.9049479961	
39	229.300812	0.9245827198	
40	168.098953	0.9422636032	
41	114.937843	0.9578601718	
42	70.686508	0.9712417126	
43	36.206150	0.9822769165	
44	12.358013	0.9908357263	
45	0.0	0.9967873096	
46	0.0	1.0	$(\dot{\eta}\ \partial p/\partial\eta)=0,\ p=\pi,\ \eta=1$

Table 1 illustrates the vertical index of η levels, *A* and *B* and the definition of the staggered grid used in ALADIN-AUSTRIA.

The exact discrete form of surface pressure tendency $\frac{\partial \pi}{\partial t}$, advecting vertical velocity $\dot{\eta} \frac{\partial p}{\partial \eta}$, vertical advection of Q $\left(\left(\dot{\eta} \frac{\partial p}{\partial \eta}\right) \frac{\partial Q}{\partial p}\right)$, the hydrostatic equation Eq. (13), pressure force $RT \nabla \ln p + \nabla \phi$, and pressure vertical velocity ω used in ALADIN can be found in Joly (1992).

2.4 Lateral Boundary Conditions (LBC) and Coupling

The numerical treatment of the lateral boundaries is a problematic but important aspect of a limited area forecast model. The problem in the interior of the domain is well posed only when the proper set of boundary conditions is prescribed. The solution in the interior may be quite different for apparently minor variations in the boundary conditions.

In order to take into account effects due to weather processes evolving outside the model domain, ALADIN-AUSTRIA is coupled to the global ARPEGE model, which provides LBCs for ALADIN-AUSTRIA in a 3-hourly interval. A schematic description of the coupling preocedure between ALADIN-AUSTRIA and ARPEGE is shown in Fig. 6. The preparation of the ARPEGE field to ALADIN LBC's is exactly the same as for the ALADIN initial conditions, which is described in detail in Section 2.6.

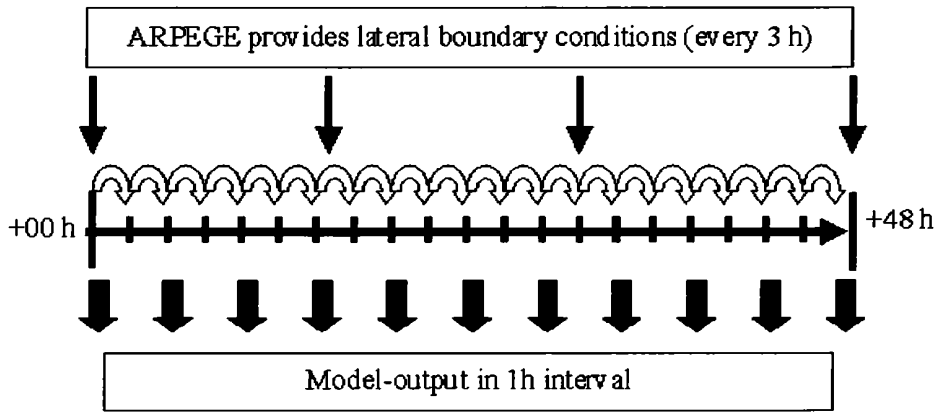

Figure 6: Schematic illustration of the coupling between ALADIN-AUSTRIA and ARPEGE.

If meteorological fields from a large scale model such as ARPEGE are to be used, three problems need to be solved.

---- Since ALADIN is a limited area spectral model, the fields used on the boundary must be double-periodic both in x and y directions in order to enable the Fourier transformation for the calculation of the derivatives.

---- If the forecasted values from ARPEGE are not consistent with the values near the boundary predicted by ALADIN, noise in the forecast variables will develop near the boundaries. This undesirable numerical noise should be suppressed at the boundaries of the domain of interest **C**.

---- ARPEGE forecasts have to be imposed on the **I** and **E** parts of the model domain in order to take into account the processes evolving out side the domain of the interest.

The solutions to those above mentioned problems in ALADIN-AUSTRIA are the doubly-periodicisation operation and the relaxation technique for coupling, which is effective in removing the artificial reflection and transmission of small scale waves on the boundaries of the domain of interest **C**.

As the doubly-periodicisation operator in ALADIN-AUSTRIA, cubic spline functions are used with subsequent Laplacian transversal smoothing. This ensures continuous derivatives up to second order, isotropy and no unrealistic overshooting (Horányi et al., 1996)

The coupling method used in ALADIN-AUSTRIA is the relaxation technique proposed by Davies (1976):

$$X^A = (1-\alpha)X^0 + \alpha X^C, \tag{26}$$

where X^A refers to the value in the **I**-zone after coupling, X^C is the value from the large scale model ARPEGE and X^0 corresponds to the value before coupling. α is the relaxation coefficent, its value is 0 for the **C**-zone, varies between 0 and 1 for the **I**-zone and is 1 for the **E**-zone. α is calculated from a special differentiable function (Janiskova, 1994). Radnoti (1995) discussed some specific aspects of the coupling strategy in ALADIN.

2.5 Temporal differencing: the semi-Lagrangian semi-implicit (SLSI) scheme

The time-integration scheme in ALADIN-AUSTRIA is a semi-Lagrangian scheme including a semi-implicit correction, which allows for a time step much larger than allowed by the CFL (Courant-Friedrichs-Levy) criterion. The key to the stability of the scheme is the removal of fast-propagating and possibly fast-advecting processes in the semi-implicit correction. For variable X at time t, the explicit leap-frog scheme in an Eulerian model can be written as:

$$\frac{X^+ - X^-}{2\Delta t} = D(X) \tag{27}$$

where X^+ is X at time $t+\Delta t$ and X^- is X at time $t-\Delta t$. D includes the physical processes in the model like energy conversions, advection or wave propagation. Separating the linear or nearly linear processes L from those in D and introducing the semi-implicit coefficient β, we have

$$\frac{X^+ - X^-}{2\Delta t} = D(X) + \beta L\left(\frac{1}{2}(X^+ + X^-) - X\right). \tag{28}$$

Noting the linearity of L, Eq. (28) can be expressed as

$$(I - \beta\Delta t L)X^+ = X^+_{EXPLICIT} + \beta\Delta t L(X^- - 2X). \tag{29}$$

The inversion of the matrix on the left-hand of the equation (I is the unit matrix) is the price to pay for the larger time step. The inversion is done in spectral space as it involves the inversion of a Laplacian operator, which is the so called implicit part of the semi-implicit correction. The first term on the right hand of the Eq. (29), $X^+_{EXPLICIT}$, is the first guess of X^+ given by the explicit integration of Eq. (27). The second term, the explicit part of the semi-implicit correction, is computed in the real, physical space. The physical processes including the fast propagating gravity waves must be in the linear operator L in order to enhance the computational stability. The detailed technical description of the scheme in ALADIN, such as the definition of the operator L, is given by Joly (1992).

The semi-Lagrangian scheme allows a further increase of the time step because of the unconditionally stable advection part of the model. There is no more constraint on the time step by the CFL stability conditions. The ALADIN semi-Lagrangian scheme originated from ARPEGE. Some modifications were needed, however, due to the plane geometry and the limited area character. It has the following features:

- three dimensional
- two-time level
- pseudo second order de-centering
- 32 grid points linear/cubic interpolation

Again, for the variable X:

$$\frac{dX}{dt} = L + N + P \tag{30}$$

where L, N and P represent linear, non-linear and physical forcing terms, respectively. The semi-implicit semi-Lagrangian algorithm of the equation can then be written as

$$\frac{X_G^{t+1} - X_O^t}{2\Delta t} = (1+\varepsilon)\left(\frac{L(X_O^t) + L(X_G^{t+1})}{2}\right) - \varepsilon L(X_M^{t+1/2}) + N(X_M^{t+1/2}) + P(X_O^t), \tag{31}$$

where

$$X^{t+1/2} = (3X^t - X^{t-1})/2 \tag{32}$$

and ε is called the de-centering parameter. G is the grid point, O is the origin and M is the middle of the $O \rightarrow G$ trajectory.

The well-known problem of orographic resonance in the SLSI scheme (Coiffier et al., 1987) is solved in ALADIN *a)* by using the de-centering in the semi-implicit algorithm in order to have it more implicit, because the orographic resonant waves are stationary gravity waves in nature, and *b)* by increasing the "divergence damping" in the horizontal diffusion, because a flow that is likely to enter into resonance is obviously divergent.

For ALADIN, special attention must be paid to the computation of trajectories originating in the extension zone. There is a necessity of having grid-point calculations also in the extension zone for coupling and doubly-periodization for the spectral transformation, but the values of prognostic variables in the **E** zone are physically meaningless. The computation of trajectories near the edge of the **C+I** domain, which may originate in the **E** zone, is carried out by assuming that the values of the prognostic variables at the origin point over E-zone are equal to the values at the nearest grid point of the **C+I** domain. Experiments in ALADIN have shown that the errors introduced by this assumption did not lead to any serious problems if the **I**-zone is sufficiently wide (8 grid points in case of ALADIN-AUSTRIA).

In ALADIN-AUSTRIA:

Time step=415.385 seconds, integration up to 48 hours, twice a day at 00 and 12 UTC

2.6 Initial Condition and Digital Filter Initialisation (DFI)

2.6.1 Initial Condition

Within the international cooperation, an ALADIN 3D-VAR data assimilation scheme has been developed (Fisher, 2002). Assimilation experiments have been carried out using data from many different observing systems such as TEMP, SYNOP, MSG, SATOB, SHIP, ATOVS, AMDAR and wind profiler (Wang et al., 2004). The assimilation of radar data with ALADIN-3DVAR is under development. As the results have not yet been too encouraging ZAMG still keeps the dynamical adaptation option, which means that the initial condition of the model ALADIN-AUSTRIA is obtained by interpolation from the global model ARPEGE analyses. The following sequence of operations is performed:

A. Transformation of global spectral fields from spherical harmonics to the co-location grid.
B. Horizontal interpolation with a bi-linear or a 12-point cubic Lagrangian polynomials interpolation.
C. Doubly-periodicization.
D. Vertical interpolation.
E. Transformation of the grid point fields into full harmonics.

The most important option in running the horizontal interpolation is the capability of using departure between the climatological mean values and the surface prognostic fields. This option ensures to have small-scale details in the interpolated data (Horányi et al., 1996). Concerning the vertical interpolation,

a displacement of the planetary boundary layer (PBL) has been implemented in order to keep its structure as much as possible. For this method an intermediate vertical system is created firstly which is defined by a special combination of the characteristics of the input and target systems. The next step is the vertical interpolation from the input and the intermediate systems to the target one using a weighting function varying between 0 and 1 and which ensures a smooth transition in the PBL transition layer. Below this transition zone the results of the intermediate system are taken individually and above only the original one is considered (Bubnova et al., 1993).

The parameters in the initial condition for ALADIN-AUSTRIA can be listed as follows:

3D: *wind, temperature, specific humidity.*

2D: *surface pressure, orography, surface temperature and relative moisture contents, deep soil temperature and moisture contents, snow cover, albedo, emissivity, land sea mask, proportion of vegetation, roughness length, standard deviation, anisotropy and orientation of sub-grid scale orography.*

All fields are handed over in form of spectral coefficients.

2.6.2 Digital Filter Initialisation

If the initial conditions of the model are not in an appropriate state of balance, like the wind and mass fields with each other, the unbalanced part will project onto inertia-gravity waves. These waves have large horizontal divergence and propagate horizontally. Due to the interpolation from the global to the limited area geometry in the dynamical adaptation option of ALADIN-AUSTRIA and due to the higher resolving orography in ALADIN-AUSTRIA, an unrealistic unbalance is unavoidably introduced in the initial conditions in ALADIN-AUSTRIA. This noise would raise spurious high-frequency oscillations in the forecasts and cause numerical instability at the beginning of the model integration. To remove or reduce this high frequency noise, Digital Filter Initialisation DFI (Lynch and Huang, 1992) is used in ALADIN-AUSTRIA.

The main idea of DFI is to construct a filter in order to damp the high frequency noise by considering the temporal Fourier series of the prognostic variable. The filtering weights are chosen in such a way that for low frequencies the amplitude of the solution with that frequency remains mostly unchanged, whereas for high frequencies the amplitude is substantially reduced.

The practice in ALADIN-AUSTRIA is that the uninitialized model state is integrated forward using the full model with physics from $t = 0$ to $t = t_N = N\Delta t$, and backward using dry adiabatic dynamics from $t = 0$ to $t = -t_N = -N\Delta t$ For any model field f, at every time step $t_n = n\Delta t$, $f_n\{f_{-N},...,f_{-2},f_{-1},f_0,f_1,f_2,...,f_N\}$ is known. f_n may be regarded as the Fourier coefficients of a function $F(\theta)$:

$$F(\theta) = \sum_{n=-N}^{n=N} f_n e^{-in\theta} \tag{33}$$

where θ is the *digital frequency.* High frequency components of f_n could be damped by multiplying $F(\theta)$ by a function $H(\theta)$:

$$H(\theta) = \frac{T_{2N}[x_0 \cos(\theta/2)]}{T_{2N}(x_0)} \tag{34}$$

where $x_0 = \frac{1}{\cos\left(\frac{\Theta_c}{2}\right)}$, Θ_c is the *cutoff frequency*. T_{2N} is a Dolph – Tchebychev polynomial, which is defined as:

$$T_n(x) = \begin{cases} \cos(n\cos^{-1} x) & if|x| \le 1 \\ \cosh(n\cosh^{-1} x) & if|x| > 1 \end{cases} \tag{35}$$

resulting in $T_0(x) = 1$ and $T_1(x) = x$. The higher polynomials can be obtained from the recurrence relationship

$$T_n(x) = 2xT_{n-1}(x) - T_{n-2(x)} \qquad n \ge 2 \tag{36}$$

For the low-frequency range, $H(\theta)$ decreases from 1 to $r = \frac{1}{T_{2N}(x_0)}$ as $|\Theta|$ goes from 0 to Θ_c, and for the high frequency range $\Theta_c \le |\Theta \le \pi|$, $H(\theta)$ oscillates within $\pm r$. Let f_n^* denote the low-frequency part of f_n, clearly:

$$H(\theta)\cdot F(\theta) = \sum_{n=-N}^{n=N} f_n^* e^{-in\theta} \tag{37}$$

and

$$f_n^* = \sum_{k=-N}^{k=N} (H\cdot F)_k f_{n-k} = \sum_{k=-N}^{k=N} h_k f_{n-k} \tag{38}$$

In ALADIN-AUSTRIA we choose $N = 20$, $\Theta_c = \frac{\pi}{30}$, and h_n is given by:

$$h_n = \frac{1}{2N+1}\left[1 + 2r\sum_{m=1}^{N} T_{2N}(x_0 \cos\frac{\theta_m}{2})\cos m\theta_n\right] \tag{39}$$

The solution of the model, integrated from $-t_N$ to t_N, is weighted averaged:

$$f^*(0) = \sum_{n=-N}^{N} h_n f_n \tag{40}$$

so that at the end of the DFI a balance is achieved in the initial state fields.

2.7 Horizontal Diffusion

Horizontal diffusion is necessary in the model to control non-linear instability and to help reducing errors introduced through aliasing. A highly selective 4^{th}-order horizontal diffusion is used in ALADIN-AUSTRIA.

$$\left(\frac{\partial X}{\partial t}\right)_{hdiff} = -K(r,l)\nabla^2\left(\nabla^2 X^{t-1}\right) \tag{41}$$

where K is the diffusion coefficient. It takes the form:

$$K \propto \frac{y_0 r^4}{\min(y_0, p_{st}(l)/p_{ref})} \tag{42}$$

$$r = \sqrt{\left(\frac{n}{N}\right)^2 + \left(\frac{m}{M}\right)^2} \tag{43}$$

where r is the relative wave number, and l is the vertical level, p_{st} is the pressure of the standard atmosphere at level l and p_{ref} the reference pressure of the same standard atmosphere. y_0 is a tuning parameter with values between *0* and *1*.

The coefficients K are the same for vorticity, specific humidity and temperature, and by a factor *9* larger for divergence (a translation to spectral horizontal diffusion of the finite difference "divergence damping"). There is no diffusion of surface pressure. To reduce spurious diffusive fluxes along slopes in the vicinity of steep mountains, it is not T but $T - \beta \ln(\pi)$ which is diffused, where β is a constant depending on the vertical level. A detailed description of the horizontal diffusion in ALADIN can be found in Geleyn (1998) and Yessad (2004).

2.8 Physical parameterizations

The parameterization of processes that are not explicitly modelled represents a major source of forecast uncertainty and is an area of intense research within the NWP community. Parameterization techniques must be employed whenever a process is (a) too small-scale to be modelled explicitly, or (b) too little understood in detail. Usually both (a) and (b) apply, which means the coefficients of a parameterization have to be tuned empirically. Today's NWP models such as ALADIN employ one-dimensional physics, that is, each model column is treated independently. Exchanges between columns takes place via dynamics and horizontal diffusion only. This simplification, which also allows for efficient parallelization, will no longer be justified in the future, especially over complex terrain, when the grid spacing of NWP models will be reduced towards 2-3 km. The following description is mainly based on the physics documentation by Gerard (2000), and on a summary given by Geleyn (2003) of physics parameterizations in ALADIN. Several aspects of ALADIN model physics can also be found in Geleyn (1998).

2.8.1 Radiation

Radiation calculations put a heavy burden on any NWP model simulation, expecially in the longwave part of the spectrum where each atmospheric layer exchanges radiation with each other layer, and with the Earth's surface. The scheme used in ALADIN-AUSTRIA is based on Geleyn and Hollingsworth (1979) and Ritter and Geleyn (1991). It is numerically relatively economical and thus can be called at each time-step. It has one spectral interval in the solar as well as in the thermal range, considers all active gases, and distinguishes between liquid and ice phase effects in clouds. It uses a

grey-body approach, which means that radiation emission and absorption is handled through bulk emissivities over the whole shortwave and longwave spectral ranges, respectively. It also makes use of Eddington's approximation which says that isotropy allows to describe the radiation field with one upward and one downward flux only. A third flux represents parallel solar radiation.

$$\frac{\partial F_\nu^\uparrow}{\partial \delta_\nu} = 2\pi(1-\omega_\nu)B_\nu(T) + \omega_\nu(1-\beta_0)\frac{S_\nu}{\mu_0}e^{-\frac{\delta_\nu}{\mu_0}} - 2[1-\omega_\nu(1-\beta)]F_\nu^\downarrow + 2\omega_\nu\beta F_\nu^\uparrow \tag{44}$$

$$\frac{\partial F_\nu^\downarrow}{\partial \delta_\nu} = -2\pi(1-\omega_\nu)B_\nu(T) - \omega_\nu\beta_0\frac{S_\nu}{\mu_0}e^{-\frac{\delta_\nu}{\mu_0}} + 2[1-\omega_\nu(1-\beta)]F_\nu^\downarrow - 2\omega_\nu\beta F_\nu^\uparrow \tag{45}$$

$$\frac{\partial S_\nu}{\partial \delta_\nu} = -\frac{S_\nu}{\mu_0} \tag{46}$$

Here δ_ν is the optical depth (increasing downwards), ω_ν is the single scattering albedo, and β is a diffusivity factor, representing the back-scattered fraction of diffuse radiation, whereas β_0 is the fraction of solar radiation that is back-scattered upwards. The cosine of the solar zenith angle is denoted by μ_0, and $B_\nu(T)$ denotes the Planck source function for thermal radiation. The subscript ν indicates frequency-dependency. In the model, Eqs. (44) - (46) are used in spectrally integrated form. Neglecting variations of $B_\nu(T)$ within model layers, the spectral integration can be separated from the vertical integration, and Stefan's law

$$B(T) = \int_0^\infty B_\nu(T)d\nu = \sigma T^4 \tag{47}$$

can be applied, where σ is Stefan's constant. The optical depth δ_ν and the single scattering albedo ω_ν depend on coefficients which characterize absorption by constituents approximated as grey bodies (aerosols, clouds) and on the spectral absorption coefficients for the gases H_2O, CO_2, and O_3. In practice, δ_ν is computed by a summation of contributions from finite frequency intervals $\Delta\nu$ given by

$$\Delta\delta_{\Delta\nu} = k_{\Delta\nu}u_{grey}, \tag{48}$$

where $u_{grey} = q_{grey}\Delta p$ is the quantity of the given grey body (liquid water, ice, aerosol) over the depth of the layer, and $k_{\Delta\nu}$ is a mean spectral coefficient for the frequency interval. For partially cloudy layers it is assumed that (a) each cloud extends over the whole layer depth, (b) the cloud fraction is constant over the layer, (c) there is no lateral effect between clouds and clear sky. The vertical flux divergence computed in the radiation scheme then enters, together with other diabatic contributions, the r.h.s. of the thermodynamic tendency equation (20).

2.8.2 Turbulent transport and surface exchange

Turbulent fluxes of momentum, heat and water vapour are modelled using a first-order turbulence closure (Louis, 1979; Louis et al., 1982). The turbulent diffusivity of a quantity ψ is determined via a diagnostic relationship as a function of wind shear and Richardson number

$$K_\psi = l_m l_\psi \left|\frac{\partial \vec{V}}{\partial z}\right| f(Ri) \tag{49}$$

where l_ψ and l_m denote mixing lengths for the given quantity, and momentum, respectively. The scheme contains a modification proposed by Geleyn (1987) which takes into account the enhancing effect of shallow convection on vertical transport. During recent years much effort has been spent on improving the scheme's dependency on Ri in the stably stratified case. Two critical Richardson numbers have been introduced, dealing with the enhancing effect of sub-grid inhomogeneity on fluxes, and with differences in behaviour between thermal and momentum fluxes.

Above the lowest model level, turbulent vertical fluxes of the quantity ψ are computed from diffusivities given by (49) through a finite-difference form of the flux-gradient relationship

$$J_\psi = -g\rho K_\psi \frac{\Delta\psi}{\Delta p}. \tag{50}$$

At the surface, fluxes are parameterized using the aerodynamic formulation

$$J_\psi(z_0) = \rho C_\psi(Ri)\left|\vec{V}(z_0)\right|(\psi(z_0) - \psi_s), \tag{51}$$

where z_0 is the lowest model level, and the subscript *s* denotes the surface value of the variable Ψ.

2.8.3 Cloudiness and large-scale precipitation

The cloudiness scheme of ALADIN-AUSTRIA is diagnostic. Explicitly resolved cloudiness and cloud water content are determined simply as a function of humidity and temperature. Stratiform cloud water content (with the dimension of a specific humidity) is computed from

$$q_s = (q_s)_{\max}\left(1 - e^{-\alpha\Delta q/(q_s)_{\max}}\right) \tag{52}$$

where the specific humidity pseudo-supersaturation is given by

$$\Delta q = q - r_c q_{SAT}. \tag{53}$$

The critical relative humidity r_c is prescribed as a vertical profile. It is close to 1 at the bottom and top of the atmosphere, and has a minimum ad mid-tropospheric levels. The negative-exponential form of (52) takes into account the fact that with increasing cloud water content smaller and smaller proportions of newly condensed water remain in the cloud. Stratiform cloud fraction n_s is estimated from stratiform cloud water content through an empirical relationship. Convective cloud water content q_c and cloud fraction n_c are diagnosed as a function of the vertical divergence of precipitation flux computed in the deep convection scheme. The final combination of stratiform and convective contributions gives

$$q_{tot} = q_s + q_c, \tag{54}$$

$$n_{tot} = n_s + (1 - n_s)n_c. \tag{55}$$

The precipitation flux is computed from the condensation rates at each level assuming that any supersaturation is instantly transformed into precipitation, taking into account sub-cloud evaporation, melting, and freezing with a revised Kessler (1969) scheme.

While the above scheme assumes that condensate is immediately converted into precipitation, starting with Cycle 29 of the ALADIN model there is an option to use the Lopez microphysical parameterization, which allows cloud water and cloud ice to be treated more explicitly (Lopez, 2002). In this scheme, microphysical conversion terms such as autoconversion and accretion are parameterized, and cloud water and ice are treated as prognostic variables that can undergo storage and depletion and can be adevcted with the flow. Tests on orographic precipitation cases show that the prognostic scheme

eliminates some of the systematic errors which were present in the diagnostic scheme, such as the 'dry valley' problem associated with excessive rain-out on upwind mountain slopes and ridges.

2.8.4 Deep convection

The parameterization of deep convection in ALADIN-AUSTRIA is based on the mass-flux-type scheme of Bougeault (1985) but has been refined in several respects. The Kuo-type closure has been made resolution-dependent following the ideas of Bougeault and Geleyn (1989). A comprehensive treatment of the vertical transport of horizontal momentum was introduced (Gregory et al., 1997). The entrainment rate varies with height, following the proposal of Gregory and Rowntree (1990). This takes account of the fact that clouds which manage to grow up to a certain height have a higher buoyancy than the average clouds below. The detrainment rate contains a constant component and a component that depends on the buoyancy decrease in the upper part of the cloud. Downdrafts are parameterized in a fashion similar to the updraft computation (Ducrocq and Bougeault, 1995).
The core of any deep convection scheme is the cloud model. As in many other parameterizations, it is a single entraining updraft

$$\frac{\partial \psi_u}{\partial \phi} = -\lambda_u (\psi_u - \psi) \tag{56}$$

where the entrainment parameter λ_u determines the degree of relaxation of the saturated-adiabatic ascent within the cloud towards the environment. The variable ψ stands for potential temperature, specific humidity, or the wind vector. The second important characteristic of a deep convection scheme is its trigger function. In ALADIN-AUSTRIA, a double Kuo-type condition is used. In order for deep convection to develop at a certain level, there must be positive buoyancy as determined from the entraining ascent, and positive moisture convergence in the layers below. Moisture convergence also determines the amount of precipitation generated by the scheme.

2.8.5 Mountain drag

At a resolution of 10 km it is necessary to parameterize the effect of unresolved features in the topography on the atmospheric flow field and the associated momentum transport. The linear gravity wave drag contribution is based on the work of Boer et al. (1984) and represented by

$$\vec{\tau} = c\rho N \vec{v}_s h_s \tag{57}$$

where $\vec{\tau}$ is the vertical flux of horizontal momentum, N is the Brunt-Väisälä frequency, h_s the standard deviation of the unresolved topography, and $\vec{v}_s$ a suitable near-surface wind vector. The form drag contribution follows Lott and Miller (1997). It is based on the dividing streamline concept which describes the empirical fact that the airflow over an obstacle tends to split into two distinct regions. At low levels, due to stability, the flow may be blocked or flow around the obstacle with little vertical motion. The Froude number determines the depth of the lower layer. Effects due to the anistropy of the sub-grid topography are parameterized as in Phillips (1984).

2.8.6 Soil processes

The treatment of soil processes is based on the ISBA (Interactions Soil Biosphere Atmosphere) scheme described by Noilhan and Planton (1989) and Giard and Bazile (2000). It uses 6 prognostic variables: surface temperature, deep soil temperature, surface reservoir water content, deep reservoir water content, interception reservoir water content, and the water content of the snow cover. Physical characteristics include vegetation fraction, land-use type (sea, ice, low vegetation or desert, high vegetation), minimum surface resistance, clay and sand percentages, active soil depth, leaf-area index, and thermal roughness length. Recent modifications of the scheme take into account the freezing-melting effects of soil water at different levels.

3. Results: Verification and case studies

3.1 Verification of ALADIN-AUSTRIA

For the present study, we performed a two months parallel suite of ALADIN-AUSTRIA from 20 Feb 2004 to 20 Apr 2004. To verify the results of ALADIN-AUSTRIA, the model's analysis fields (12h interval) were used for upper air parameters and SYNOP observations for the near surface parameters. Verification results of ALADIN-LACE, ALADIN-VIENNA and ALALDIN-AUSTRIA were compared in order to assess the performance of ALADIN-AUSTRIA.

a) Verification of upper air fields

In Fig. 7, Fig. 8 and Fig. 9, we compare the time series of domain means of BIAS and RMSE of the ALADIN-LACE and ALADIN-AUSTRIA 24h and 48h forecasts of 500hPa geopotential. The ALADIN configurations AUSTRIA and LACE behave similarly, but a slight improvement with ALADIN-AUSTRIA is observed at longer forecast periods (forecast range 48h), at least regarding the BIAS (Fig. 8).

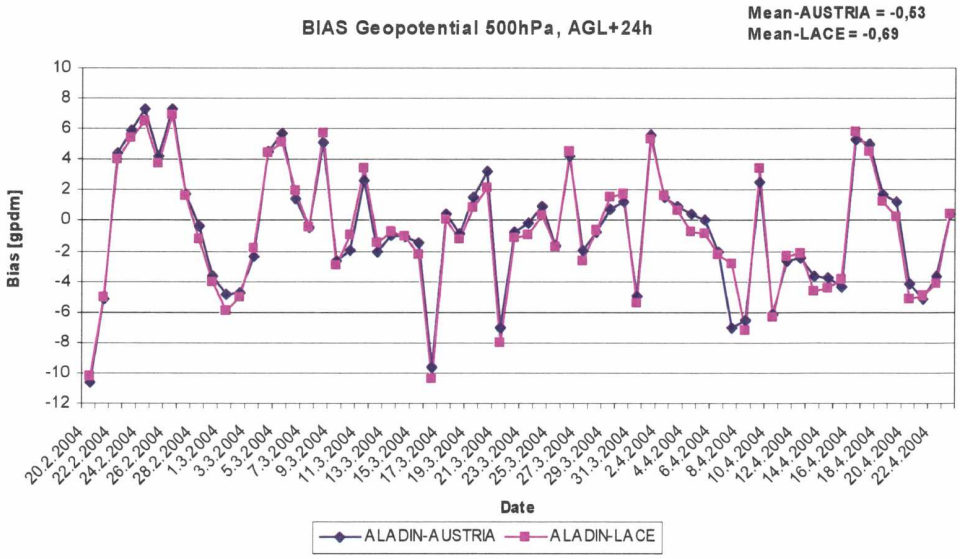

Figure 7: Bias of 500hPa geopotential, 24h forecast, with mean values given at the upper right. Blue line: ALADIN-AUSTRIA, red line: ALADIN-LACE.

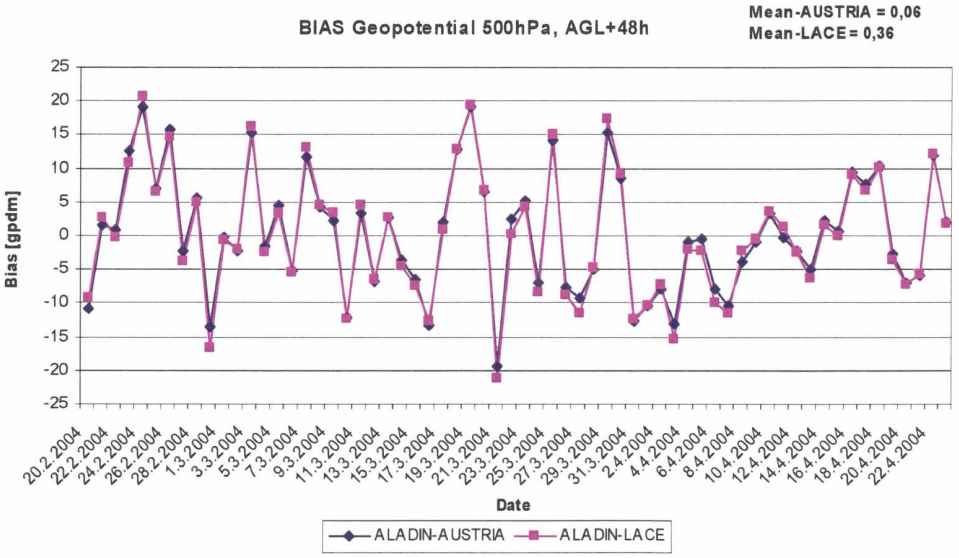

Figure 8: Bias of 500hPa geopotential, 48h forecast, with mean values given at the upper right. Blue line: ALADIN-AUSTRIA, red line: ALADIN-LACE.

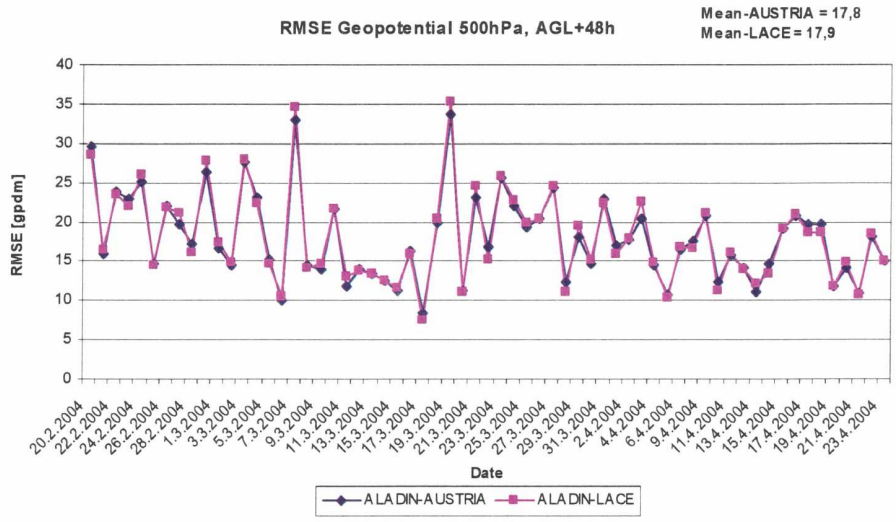

Figure 9: Same as Fig. 8, but for RMSE of 500hPa geopotential, 48h forecast.

b) Verification of surface fields

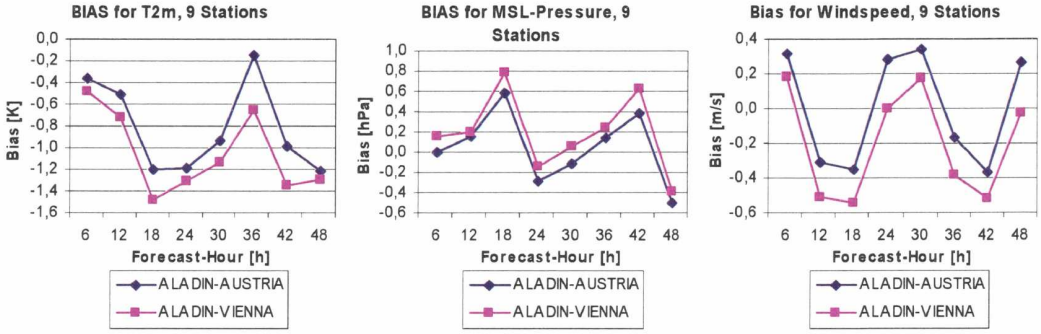

Figure 10: BIAS of T2m, MSL-pressure, wind speed (averaged over 9 major Austrian cities), blue: ALADIN-AUSTRIA; red: ALADIN-VIENNA.

Verification of surface fields was done for 2m temperature, MSL pressure and 10m wind speed for 9 major Austrian cities. Fig. 10 shows a comparison between ALADIN-AUSTRIA and ALADIN-VIENNA for the averaged BIAS over the 9 cities. For 2m temperature, BIAS and RMSE are reduced by 10% in ALADIN-AUSTRIA. Errors of wind speed do not differ much between ALADIN-AUSTRIA and ALADIN-LACE. Focusing on the verification of station Vienna, which is shown in Fig. 11, the slight improvement of the 2m temperature and MSL pressure forecast is confirmed, whereas the quality of the wind speed forecast remains rather unchanged.

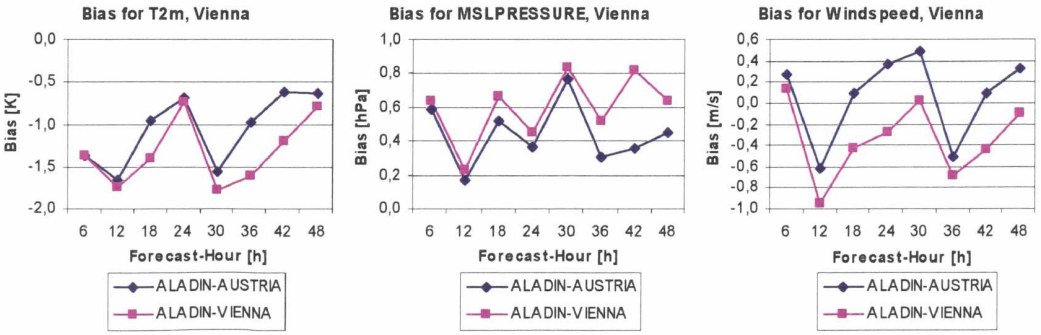

Figure 11: BIAS of T2m, MSL-pressure, wind speed for station Vienna, line in blue: ALADIN-AUSTRIA; in red: ALADIN-VIENNA.

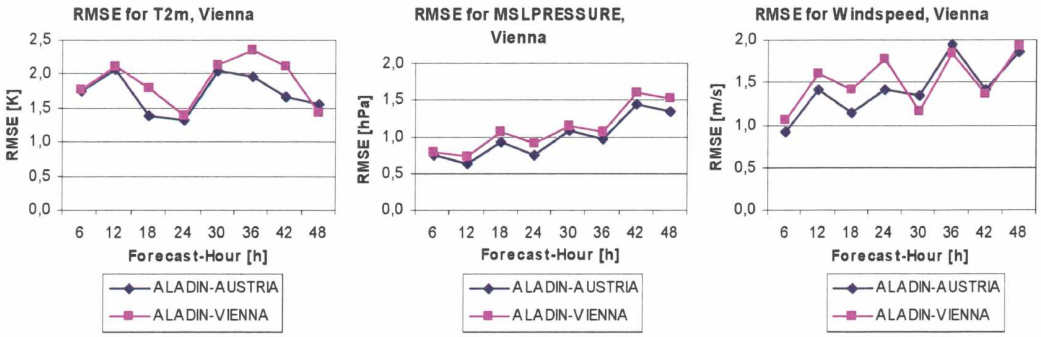

Figure 12: Same as Fig.11, but for RMSE.

3.2 Case study

It has been observed that during the summer season ALADIN produces light to moderate convective rainfall when none, or significantly less, was observed. The unrealistic convective rainfall is widespread and strongly tied to orographic features such as the main alpine crest. Wimmer (2004) has investigated the problem using different representations of model orography and convection schemes in ALADIN-VIENNA and ALADIN-AUSTRIA. One of the case studies aimed at evaluating the impact of model resolution on convective rainfall. One of his findings is that ALADIN-AUSTRIA brings a beneficial effect on convective rainfall and its triggering. To demonstrate this improvement, we compare the forecasts of accumulated convective rainfall of ALADIN-VIENNA and ALADIN-AUSTRIA, which is shown in Fig. 13. On the 6th of May 2003, there was no convective precipitation observed between 00UTC and 18UTC in the western parts of Austria. In the forecast of ALADIN-VIENNA, unrealistic and widespread convective rainfall was found over the mountains in the region. With higher vertical resolution in ALADIN-AUSTRIA, the intensity and areal extension of the convective rainfall cells are significantly reduced.

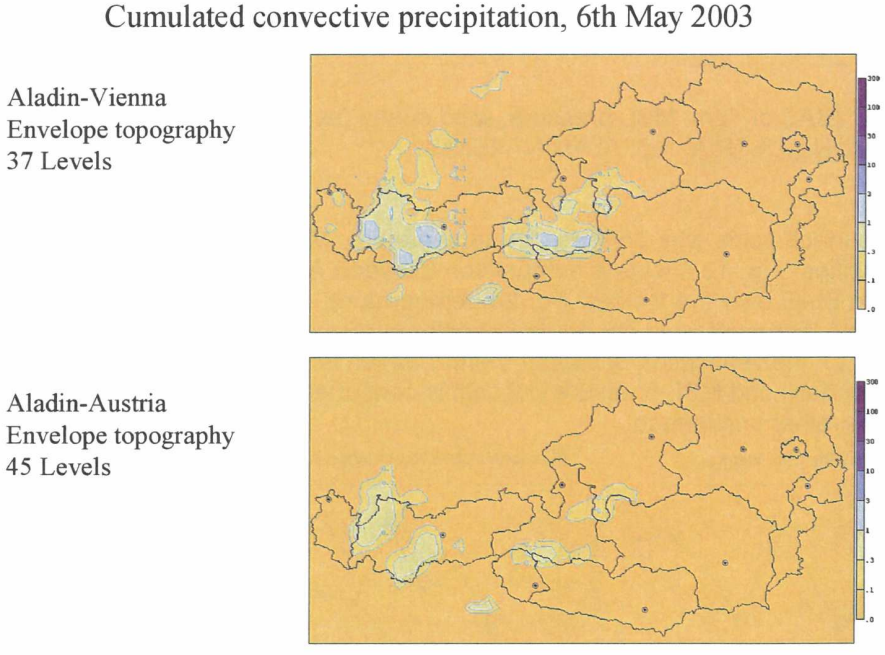

Figure 13: Forecasts of accumulated convective rainfall with ALADIN-VIENNA and ALADIN-AUSTRIA. Both models started at 00 UTC, 6. May 2003. The forecasts are valid from 00UTC to 18 UTC, 6. May 2003.

4. Conclusions and Future Plans

Since 1998 the numerical limited area prediction system ALADIN has been in use operationally at ZAMG. The performance of the system in the last years is shown in Figs. 14-17, which give anomaly correlation, Bias, Mean Absolute Error, Root Mean Square Error, and Standard Deviation Error of 48h forecast of 500hPa geopotential (Fig. 14 and Fig. 15) and of 24h forecast of 500hPa geopotential (Fig. 16 and Fig. 17).

In order to improve the forecast quality, to use the available computer power more efficiently, and simplify the operational production procedure of NWP at ZAMG, the new NWP-LAM system ALADIN-AUSTRIA was designed. The new system combines its two predecessors ALADIN-VIENNA and ALADIN-LACE into a single Central European domain, keeps the higher horizontal resolution (9.6 km), and increases the vertical resolution from 37 to 45 levels. The main features of ALALDIN-AUSTRIA have been summarized in Table 2.

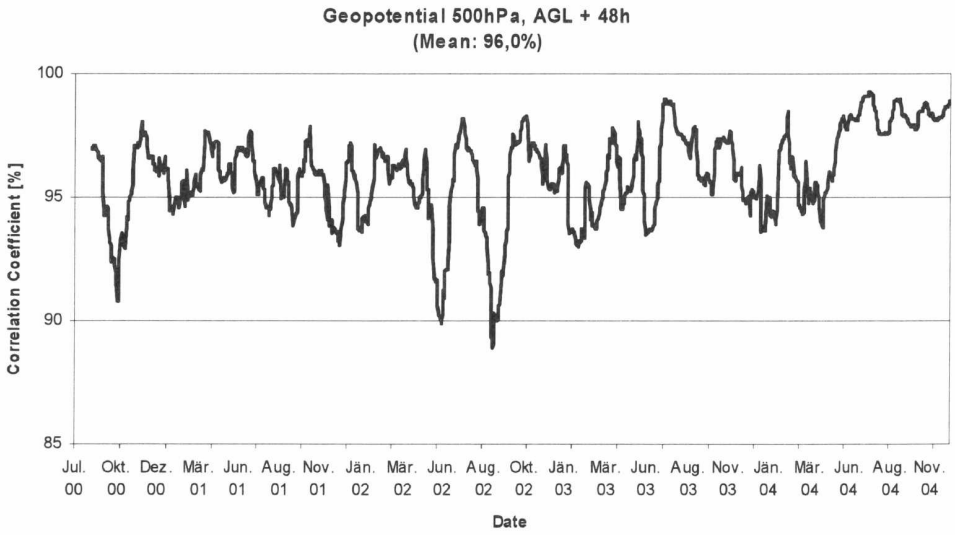

Figure 14: Anomaly correlation of 48h forecast of 500hPa geopotential since August 2000. Forecast system: ALADIN-VIENNA up to 09 May 2004, ALADIN-AUSTRIA, after 10.May 2004

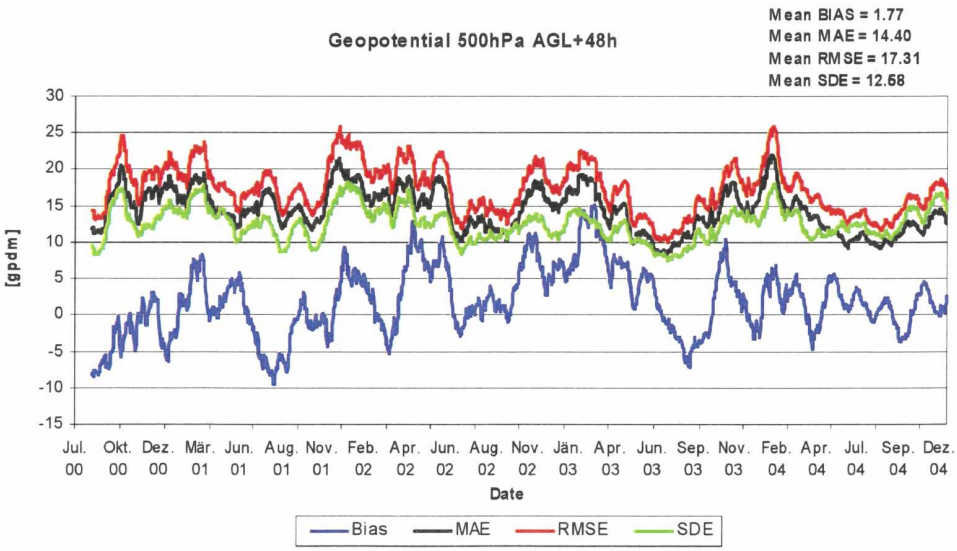

Figure 15: Same as Fig. 14, but for Bias, MAE, RMSE and SDE.

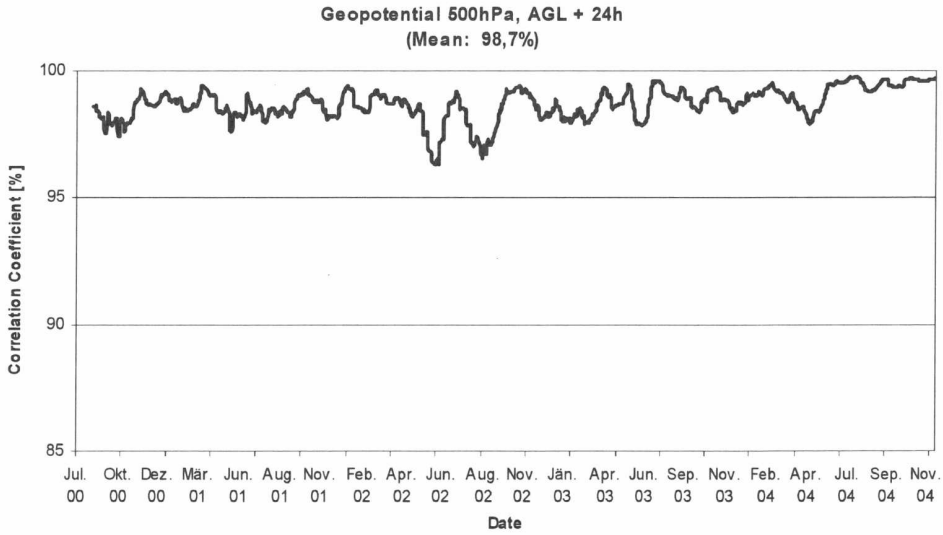

Figure 16: Anomaly correlation of 24h forecast of 500hPa geopotential since August 2000. Forecast system: ALADIN-VIENNA up to 09 May 2004, ALADIN-AUSTRIA, after 10.May 2004

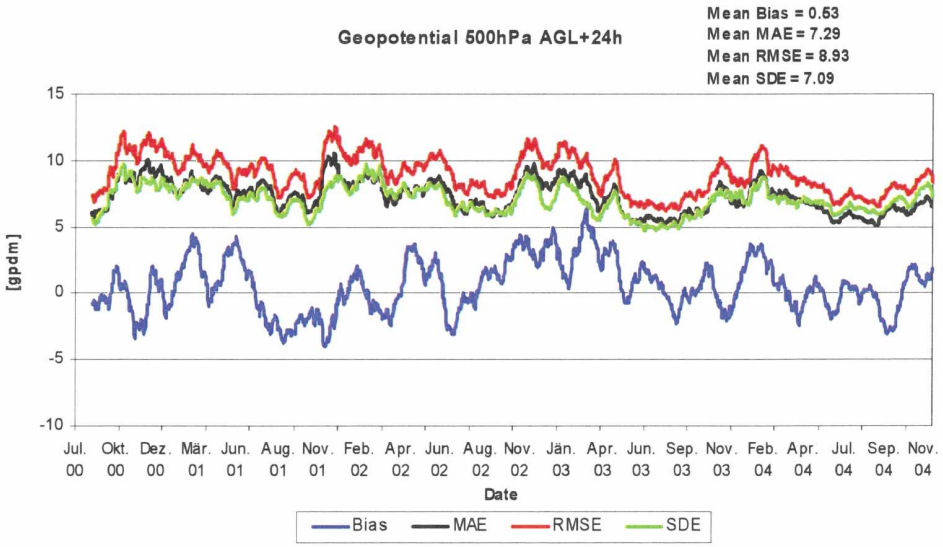

Figure 17: Same as Fig. 16, but for Bias, MAE, RMSE and SDE.

A two months parallel run from 20 Feb 2004 to 20 April 2004 was carried out investigating the performance of ALADIN-AUSTRIA as compared to ALADIN-VIENNA and ALADIN-LACE. Model analyses were used to verify upper-air parameters, and SYNOP observation for the near surface forecast. Verification statistics show a slight improvement, specifically for near surface forecasts such as 2m temperature and for upper air parameters at the longer forecast range. The quality of wind speed forecasts remains rather the same as in ALADIN-VIENNA.

ALADIN forecasts often produce spurious convective precipitation over complex topography. A sensitivity study of the effect of model resolution on convective precipitation was performed, in which the forecast of convective precipitation with ALADIN-AUSTRIA is compared to the one with ALADIN-VIENNA. The results of the case study show that the increase of levels in ALADIN-AUSTRIA leads to a beneficial effect on convective rainfall and its triggering.

ALADIN-AUSTRIA has been in operational use since 10 May 2004. It is evident that its resolution, the description of the atmospheric dynamics and physics, and its data assimilation system are still needed to be improved in order to provide more accurate weather prediction, for example in the forecast of strong convective events. There are several NWP research and development projects going on at ZAMG of which especially the following two should be mentioned.

Forecast Range	48 Hours
Initial Time of Model Runs	00 UTC, 12 UTC
Operating Time for 48h Forecast	Approx. 90 min. (real time)
Model Type	Spectral, Arakawa-A grid
Model Domain	Central Europe, ca. 2780 x 2500 km^2
Horizontal Resolution	9.6 km
Numbers of Grid-points in *x*- and y-direction	300 x 270
Representation of Orography	Envelope
Maximum Height of the Alpine	3553 m
Vertical Coordinate	Pressure based Hybrid Coordinate
Vertical Resolution	45 Layers
The Lowest Level	Approx. 14 m above Ground
Below 1000 m	9 Levels
1000 m to 2000 m	4 Levels
2000 m to 10000 m	17 Levels
Above 10000 m	15 Levels
Model Equations	Hydrostatic
Time Integration	SISL Semi-Implicit Semi-Lagrangian
Time Step	415 Seconds
Initial State	Interpolated from ARPEGE, DFI
Lateral Boundary Conditions	Coupled with ARPEGE at 3h Intervals
Computation of convective Tendency	At every Time Step
Computation of Radiation Cycle	Every Hour
Direct Model Output	At Every Hour
Status	Operational since 10 May 2004
Hardware	SGI-3400 (using 26 of 28 processors)

Table 2: Main features of ALADIN-AUSTRIA

I. AROME (Application of Research to Operations at MEsoscale)

The aim of the project AROME (Bouttier 2003) is to develop a new LAM based on the models ALADIN and Meso-NH, in order to improve significantly the quality of the forecast, especially weather phenomena at small scale such as strong convection ('high impact weather'). Fundamental ingredients of the model AROME are the ALADIN non-hydrostatic dynamics (Bubnová 1995 and Bénard 2004), the Meso-NH physical package (Lafore et al. 1998, Caniaux et al. 1994, Cuxart et al. 2000, Masson 2000, Pinty 1998) and the ALADIN variational data assimilation system (Fischer 2002). The main features of AROME are:

- 2-3 km horizontal resolution, 80 vertical levels, non-hydrostatic.
- Explicit convection, 3-dimensional turbulence, prognostic TKE, sophisticated microphysics with prognostic cloud water, different phase change among cloud liquid water, ice, graupel, precipitating rain, snow, hail and so on. 3-dimensional radiation effects, such as shading in mountainous area, very detailed representation of surface characteristics, including cities.
- 4D-Var rapid cycle data assimilation at a temporal resolution between 10 and 60 min. Radar data, satellite radiance and cloud products, microwave and scatterometer data, GPS, AMDAR, surface automated network are to be ingested.

II. ALADIN LAEF (Limited Area Ensemble Forecasting)

Scientific and computational limitations prevent us from constructing a perfect NWP model. Small errors in the initial condition can grow exponentially and eventually render a forecast useless. In order to address this problem in the daily ALADIN forecasts, the project "ALADIN Limited Area Ensemble Forecasting" was started at ZAMG. The ensemble forecast system ALADIN is run at 16km horizontal resolution, with 31 levels in vertical. It covers Europe and most of the North Atlantic. It is an ensemble forecast system with 11 members. Up to now, work focused on the initial condition perturbation methods Breeding (Toth and Kalnay, 1997), ETKF (Ensemble Transform Kalman Filter, Bishop et al. 2001) and ET (Ensemble Transform, Bishop and Toth, 1999). Coupling with ARPEGE global EPS system PEARP has been investigated. ALADIN dynamical downscaling of PEARP has been carried out as well. Studies on model physics perturbation, coupling with different global EPS systems, and comparisons between Breeding, ETKF and ET are planned for the near future.

Acknowledgements

Special thanks to the colleagues in the NWP division at ZAMG, F. Wimmer for providing the figures of the ALADIN-AUSTRIA case study, K. Stadlbacher, H. Seidl for their helpful discussions on the model. We gratefully acknowledge all the people who have contributed to the common work of ALADIN project. G. Radnóti, A. Horányi and R. Bubnová helped us especially in many practical issues related with ALADIN. Y. Wang is grateful for the support and hospitality of the staff in Toulouse, particularly E. Bazile, F. Bouyssel, D. Giard, J.-F. Geleyn, J.-D. Gril and P. Pottier during his working stay on ALADIN in Meteo-France within the framework of bilateral cooperation between France and Austria (Program *AMADEUS*, funded by *Österreicher Austauschdienst* ÖAD, Republic of Austria). We would also like to thank the Director of ZAMG for continuous support of the ALADIN project. We appreciate the constructive comments of M. Ehrendorfer on the first draft of this paper. Co-operations with the *Institut für Meteorologie und Geophysik, Universität Wien* are kindly acknowledged.

REFERENCES

Bénard, P. 2004: Aladin/AROME dynamical core: Status and possible extension to IFS. *ECMWF Seminar Proceedings on recent developments in numerical methods for atmospheric and ocean modelling*, 6-10 September 2004 (in print).

Bishop, C., B. J. Etherton and S. J. Majumdar, 2001: Adaptive sampling with the ensemble transform Kalman Filter, Part I: Theoretical Aspects. *Mon. Wea. Rev.,* **129**, 420-436.

Bishop, C. and Z. Toth, 1999: Ensemble transformation and adaptive observations. *J. Atmos. Sci.*, **56**, 1748-1765.

Boer, G. J., N. A. McFarlane, R. Laprise, J. D. Henderson and J.-P. Blanchet, 1984: The Canadian Climate Center spectral atmospheric general circulation model. *Atmosphere-Ocean*, **22**, 397-429.

Bougeault, Ph., 1985: A simple parameterization of the large-scale effects of cumulus convection. *Mon. Wea. Rev.,* **113**, 2108-2121.

Bougeault, Ph. And J.-F. Geleyn, 1989: Some problems of closure assumption and scale dependency in the parameterization of moist deep convection for numerical weather prediction. *Meteorol. Atmos. Phys.,* **40**, 123-135.

Bouttier, F., 2003: The Arome mesoscale project. *ECMWF Seminar Proceedings on recent developments in data assimilation for atmosphee and ocean*, 8-12 September 2003, 433-447.

Bubnová, R., A. Horányi and S. Malardel, 1993: International project ARPEGE/ALADIN. *EWGLAM Newsletter*, **15**, 117-130

Bubnová, R., G. Hello, P. Bénard and J.-F. Geleyn, 1995: Integration of the fully elastic equations cast in the hydrostatic pressure terrain-following coordinate in the framework of the ARPEGE/ALADIN NWP system. *Mon. Wea. Rev.,* **123**, 515-535.

Caian, M. and J.-F. Geleyn, 1997: Some limits to the variable-mesh solution and comparison with the nested LAM solution. *Quart. J. Roy. Meteor. Soc.,* **123**, 743-766.

Caniaux, G., J.-L. Redelsperger and J.-P. Lafore, 1994: A numerical study of the stratiform region of a fast moving squall line. Part I: General description, and water and heat budgets. *J. Atmos. Sci.*, **51**, 2046-2074.

Coiffier, J., P. Chapelet and N. Marie, 1987: Study of various quasi-Lagrangian techniques for numerical models. *ECMWF Workshop Proceedings on techniques for horizontal discretization in numerical prediction models*, 2-4 November 1987, 19-46.

Coutier, P. and J.-F. Geleyn, 1988: A global numerical weather prediction model with variable resolution: Application to the shallow water equations. *Quart. J. Roy. Meteor. Soc.,* **114**, 1321-1346.

Cuxart, J., P. Bougeault and J.-L. Redelsperger, 2000: A turblence scheme allowing for mesoscale and large-eddy simulations. *Quart. J. Roy. Meteor. Soc.,* **126**, 1-30.

Davies, H. C., 1976 : A lateral boundary formulation for multi-level prediction models. *Quart. J. Roy. Meteor. Soc.,* **102**, 405-418.

Ducrocq, V. and Ph. Bougeault, 1995: Simulation of an observed squall line with a meso-beta-scale hydrostatic model. *Mon. Wea. Rev.,* **123**, 380-399.

Fischer, C., 2002: The variational computations inside ARPEGE/ALADIN: CY25T1. *Internal Documentation Note*, Meteo-France, CNRM/GMAP. Available from the authors on request.

Geleyn, J.-F. and A. Hollingsworth, 1979: An economical analytical method for the computation of the interaction between scattering and line absorption. *Beitr. Phys. Atmosph.,* **52**, 1-16.

Geleyn, J.-F., 1987: Use of a modified Richardson number for parameterizing the effect of shallow convection. *J. Meteor. Soc. Japan, WMO/IUGG NWP Syposium spezial issue,* 141-159.

Geleyn, J.-F., 1998: Adaptation of spectral methods to non-uniform mapping (global and local). *ECMWF Seminar Proceedings on recent developments in numerical methods for atmospheric modelling*, 7-11 September 1998, 226-265.

Geleyn, J.-F., 2003: Physical parameterisations in ARPEGE and ALADIN. *Internal Documentation Note*, Meteo-France, CNRM/GMAP. Available from the authors on request.

Gerard, L., 2000: Physical parameterisations in ARPEGE-ALADIN. *Internal Documentation Note*, Meteo-France, CNRM/GMAP. Available from the authors on request.

Giard, D. and E. Bazile, 2000: Implementation of a new assimilation scheme for soil and surface variables in a global NWP model. *Mon. Wea. Rev.,* **128**, 997-1015.

Gregory, D., R. Kershaw and P. M. Inness, 1997 : Parametrization of momentum transport by convection. II: tests in single column and general circulation models. *Quart. J. Roy. Meteor. Soc.,* **123**, 1153-1183.

Gregory, D. and P. R. Rowntree, 1990 : A mass flux convection scheme with representation of cloud ensemble characteristics and stability dependent closure. *Mon. Wea. Rev.,* **118**, 1483-1506.

Gustafsson, N. and A. McDonald, 1996: A comparison of the HIRLAM gridpoint and spectral semi-Lagrangian models. *Mon. Wea. Rev.,* **124**, 2008-2022.

Haugen, J. E. and B. Machenhauer, 1993: A spectral limited area formulation with time dependent boundary conditions applied to the shallow water equations. *Mon. Wea. Rev.,* **121**, 2618-2630.

Horányi, A. I. Ihász and G. Radnóti, 1996: ARPEGE/ALADIN: A numerical weather prediction model for Central-Europe with the participation of the Hungarian Meteorological service. *Quart. J. Hungarian Meteor. Service*, **100**, 277-301.

Janiskova, M., 1994: Study of coupling problem. *Note ALADIN*, Nr.: **1**, Meteo-France, CNRM/GMAP. Available from the authors on request.

Joly, A., 1992: ARPEGE/ALADIN: adiabatic model equations and algorithm. *Internal Documentation Note*, Meteo-France, CNRM/GMAP. Available from the authors on request.

Kessler, E., 1969: On distribution and continuity of water substance in atmospheric circulation. *Meteorol. Monogr.,* **10**, 84pp.

Lafore, J.-L., J. Stein, N. Asencio, P. Bougeault, V. Ducrocq, C. Fischer, P. Héreil, J.-L. Redelsperger, E. Richard and J. Vilà-Guerau de Arellano, 1998: The Meso-NH atmospheric simulation system. Part I: adiabatic formulation and control simulation. *Ann. Geophys.*, **16**, 90-109.

Lane, D. E., R. C. J. Somerville, and S. F. Iacobellis, 2000: Sensitivity of cloud and radiation parameterisations to changes in vertical resolution. *J. Climate*, **13**, 915-922.

Lindzen, R. S. and M. S. Fox-Rabinovitz, 1989: Consistent vertical and horizontal resolution. *Mon. Wea. Rev.,* **117**, 2575-2583.

Lopez, P., 2002: Implementation and validation of a new prognostic large-scale cloud and precipitation scheme for climate and data-assimilation purposes. *Quart. J. Roy. Meteor. Soc.,* **128**, 229-257.

Lott, F. and M. J. Miller, 1997: A new subgrid-scale orographic drag parameterization: Its formulation and testing. *Quart. J. Roy. Meteor. Soc.,* **123**, 101-127.

Louis, J. F., 1979 : A parametric model of vertical eddy fluxes in the atmosphere. *Bound. Layer Meteor.*, **17**, 187-202.

Louis, J. F., M. Tiedtke and J.-F. Geleyn, 1982: A short history of the PBL parameterization at ECMWF. *ECMWF Workshop Proceedings on planetary boundary layer parameterization,* 25-27 November 1981, 59-80.

Lynch, P. and X.-Y. Huang, 1992: Initialization of the HIRLAM model using a digital filter. *Mon. Wea. Rev.,* **120**, 1019-1034.

Machenhauer, B. and J. E. Haugen, 1987: Test of a spectral limited area shallow water model with time dependent lateral boundary conditions and combined normal mode/semi-Lagrangian time integration schemes. *ECMWF Workshop Proceedings on techniques for horizontal discretization in numerical prediction models*, 2-4 November 1987, 361-377.

Majewski, D., 1998: The new global Icosahedral-Hexagonal gridpoint model GME of the Deutscher Wetterdienst. *ECMWF Seminar Proceedings on recent developments in numerical methods for atmospheric modelling*, 7-11 September 1998, 172-201.

Masson, V., 2000: A physical-based scheme for the urban energy budget in atmospheric models. *Bound. Layer Meteor.* **94**, 357-397.

Noihan, J. and S. Planton, 1989: A simple parameterization of land surface processes for the meteorological models. *Mon. Wea. Rev.,* **117**, 536-549.

Pecnick, M. J. and D. Keyser, 1989: The effect of spatial resolution on the simulation of upper-tropospheric frontogenesis using a sigma-coordinate primitive equation model. *Meteor. Atmos. Phys.*, **40**, 137-149.

Persson, P. O. G. and T. T. Warner, 1991: Model generation of spurious gravity waves due to inconsistency of the vertical and horizontal resolution. *Mon. Wea. Rev.*, **119**, 917-935.

Phillips, D. S., 1984: Analytical surface pressure and drag for linear hydrostatic flow over three-dimensional elliptical mountains. *J. Atmos. Sci.*, **41**, 1073-1084.

Pinty, J.-P. and P. Jabouille, 1998: A mixed-phase cloud parameterisation for use in mesoscale non-hydrostatic model: simulations of a squall line and of orographic precipitations. *Proceedings of conference of cloud physics,* Everett, WA, USA, Amer. Meteor. Soc., Aug. 1999, 217-220.

Radnóti, G., 1995: Comments on: A spectral limited area formulation with time-dependent boundary conditions applied to the shallow water equations. *Mon. Wea. Rev.*, **123**, 3122-3123.

Ritter, B. and Geleyn, J.-F., 1991: A comprehensive radiation scheme for numerical weather prediction models with potential applications in climate simulations. *Mon. Wea. Rev.*, **120**, 303-325.

Simmons, A. and D. Burridge, 1981: An energy and angular momentum conserving vertical finite-difference scheme and hybrid vertical coordinates. *Mon. Wea. Rev.,* **109**, 758-766.

Temperton, C., 1998: An overview of recent developments in numerical methods for atmospheric modelling. *ECMWF Seminar Proceedings on recent developments in numerical methods for atmospheric modelling*, 7-11 September 1998, 1-11.

Toth, Z. and E. Kalnay, 1997: Ensemble forecasting at NECP and the breeding method. *Mon. Wea. Rev.*, **125**, 3297-3319.

Wang, Y., J. Pailleux, T. Montmerle, V. Guidard, G. Bölöni, R. Randriamapianina and Z. Sahlaoui, 2004: Impact studies performed with the Lam system ALADIN. *Proceedings of the third WMO workshop on the impact of various observing systems on numerical weather prediction*, WMO/TD No. **1228**, 249-255.

Weaver, A. T. and E. S. Sarachik, 1990: On the importance of vertical resolution in certain ocean general circulation models. *J. Phys. Oceanogr.*, **20**, 600-609.

Weaver, A. T. and P. Courtier, 2001: Correlation modelling on the sphere using a generalized diffusion equation, *Quart. J. Roy. Meteor. Soc.,* **127**, 1815-1846.

Wimmer. F., 2004: The effect of a non-envelop topography on deep convection, *14th ALADIN-Workshop*, 1-4 June 2004, Innsbruck, Austria.

Yessad, K., 2004: Horizontal diffusion computation in the cycle29 of ARPEGE/IFS, *ARPEGE documentation,* Meteo-France, CNRM/GMAP. Available from the authors on request.

Österreichische Beiträge zu Meteorologie und Geophysik

bisher erschienen:

Heft	Publ.Nr.	Fachgebiet	Autor	Titel und Umfang	Preis in Euro
1	329	Meteorologie		*Tagungsbericht EURASAP, Wien, 14.-16. Nov. 1988, Evaluation of Atmospheric Dispersion Models Applied to the Release from Chernobyl.* Wien 1989, 20 Beiträge, 198 S., 100 Abb., 17 Tab.	14,53
2	332	Geophysik		*Tagungsbericht über das 5. Internationale Alpengravimetrie Kolloquium - Graz 1989.* Herausgeber: H. LICHTENEGGER, P. STEINHAUSER und H. SÜNKEL, Wien 1989, 256 S., 100 Abb., 17 Tab.	vergriffen
3	336	Geophysik		*Schwerpunktprojekt S47-GEO: Präalpidische Kruste in Österreich, Erster Bericht.* Herausgeber: V. HÖCK und P. STEINHAUSER, Wien 1990, 15 Beiträge, 257 S., 104 Abb., 17 Tab., 23 Fotos	20,35
4	338	Meteorologie	LANZINGER, A. et al:	*Alpex-Atlas.* FWF-Projekt P6302 GEO, Wien 1991, 234 S., 23 Abb., 2 Tab., 200 Karten	18,17
5	341	Meteorologie	BÖHM, R.:	*Lufttemperaturschwankungen in Österreich seit 1775.* Wien 1992, 95 S., 34 Abb., 24 Tab.	vergriffen
6	343	Geophysik	MEURERS, B.:	*Untersuchungen zur Bestimmung und Analyse des Schwerefeldes im Hochgebirge am Beispiel der Ostalpen.* Wien 1992, 146 S., 72 Abb., 9 Tab.	11,63
7	351	Meteorologie	AUER, I.:	*Niederschlagsschwankungen in Österreich seit Beginn der instrumentellen Beobachtungen durch die Zentralanstalt für Meteorologie und Geodynamik.* Wien 1993, 73 S., 18 Abb., 5 Tab., 6 Farbkarten	23,98
8	353	Meteorologie	STOHL, A., H. KROMP-KOLB:	*Analyse der Ozonsituation im Großraum Wien.* Wien 1994, 135 Seiten, 73 Abb., 8 Tabellen	23,98
9	356	Geophysik		*Tagungsbericht über das 6. Internationale Alpengravimetrie-Kolloquium, Leoben 1993.* Herausgeber: P. STEINHAUSER und G. WALACH, Wien 1993, 251 Seiten, 146 Abb.	23,98
10	357	Meteorologie	ZWATZ-MEISE, V.:	*Contributions to Satellite and Radar Meteorology in Central Europe.* Wien 1994, 169 Seiten, 25 Farbabb., 42 SW-Abb., 13 Tab.	23,98
11	359	Geophysik	LENHARDT W. A.:	*Induzierte Seismizität unter besonderer Berücksichtigung des tiefen Bergbaus.* Wien 1995, 91 S., 53 Abb.	23,98
12	361	Meteorologie	AUER, I., R. BÖHM, N. HAMMER †, W. SCHÖNER., WIESINGER W., WINIWARTER W.:	*Glaziologische Untersuchungen im Sonnblickgebiet: Forschungs-programm Wurtenkees.* Wien 1995, 143 S., 59 SW-Abb., 13 Farbabb., 9 SW-Fotos, 47 Tab.	23,98
13	372	Meteorologie	PIRINGER, M.:	*Results of the Sodar Intercomparison Experiment at Dürnrohr, Austria.* Wien 1996	23,98
14	373	Geophysik	MEURERS, B.:	*Proceedings of the 7th International Meeting on Alpine Gravimetry, Vienna 1996.* Wien 1996	23,98
15	374	Meteorologie	RUBEL, F.:	*PIDCAP - Quick Look Precipitation Atlas.* Wien 1996	23,98

Heft	Publ.Nr.	Fachgebiet	Autor	Titel und Umfang	Preis in Euro
16	378	Meteorologie	DOBESCH, H., KURY G.:	*Wind Atlas for the Central European Countries Austria, Croatia, Czech Republic, Hungary, Slovak Republic and Slovenia,* Wien 1997	23,98
17	382	Meteorologie		*Proceedings of the 9th International Symposium on Acoustic Remote Sensing and Associated Techniques of the Atmosphere and Oceans, Vienna 1998,* 329 Seiten, Wien 1998	23,98
18	383	Meteorologie	RUBEL, F.:	*PIDCAP - Ground Truth Precipitation Atlas.* 84 Seiten, 99 Farbkarten, Wien 1998	36,34
19	384	Meteorologie		*Proceedings of the 2nd European Conference on Applied Climatologie, 19 to 23 Oct. 1998, Vienna.* CD-ROM, Wien 1998	23,98
20	387	Meteorologie		*Proceedings of the 2nd International Conference on Experiences with Automatic Weather Stations, 27 to 29 Sept. 1999, Vienna.* CD-ROM, Wien 1999	23,98
21	388	Meteorologie		*Bericht über den Workshop Umweltforschung im Hochgebirge - Ergebnisse von GAW-Dach und verwandten Projekten, 05. bis 06. Okt. 1999, Wien.* 147 Seiten, Wien 1999	23,98
22	389	Meteorologie	DOBESCH, H., H. V. TRAN:	*The Diagnostic Wind Field Model ZAWIMOD2.* 47 Seiten, 8 Farbabb., Wien 1999	23,98
23	392	Meteorologie		*Proceedings of the 26th International Conference on Alpine Meteorology; 11 to 15 Sept. 2000, Innsbruck.* CD-ROM, Wien 2000	23,98
24	395	Meteorologie	SABO, P.:	*Hochnebelprognose mittels eines objektiven Inversionsindexes für die synoptische Praxis,* 80 Seiten, Wien 2000	23,98
25	397	Meteorologie	AUER, I., R. BÖHM, W. SCHÖNER:	*Austrian long-term climate 1767-2000 - Multiple instrumental climate time series from central Europe,* 160 Seiten, 31 Farbseiten, CD-ROM, Wien 2001	25,00
26	398	Geophysik	MEURERS, B.:	*Proceedings of the 8th International Meeting on Alpine Gravimetry, Leoben 2000,* 240 Seiten, 4 Farbseiten, Wien 2001	25,00
27	399	Meteorologie		*Proceedings of the Deutsch-Österreichisch-Schweizerische Meteorologentagung; 18 to 21 Sept. 2001, Vienna.* CD-ROM, Wien 2001	25,00
28	408	Meteorologie	AUER, I., R. BÖHM, M. LEYMÜLLER, W. SCHÖNER:	*Das Klima des Sonnblicks – Klimaatlas und Klimatographie der GAW Station Sonnblick einschliesslich der umgebenden Gebirgsregion,* 305 Seiten, 130 Farbabbildungen, CD-ROM, Wien 2002	50,00
29	409	Meteorologie		*Scientific Contributions of Austria to the Mesoscale Alpine Programme (MAP),* 74 Seiten, 38 Farbseiten, Wien 2003	25,00
30	411	Meteorologie	HUBER-POCK, F.:	*Die atmosphärischen Gleichungen in den meteorologischen Koordinatensystemen,* 160 Seiten, 1 Farbseite, Wien 2003	25,00

Heft	Publ.Nr.	Fachgebiet	Autor	Titel und Umfang	Preis in Euro
31	412	Geophysik	MEURERS, B., R. PAIL:	*Proceedings of the 1st Workshop on International Gravity Field Research, Graz 2003,* 204 Seiten, 3 Farbseiten, Wien 2004	25,00
32	413	Meteorologie	BAUMANN-STANZER, K.:	*Qualitätsprüfung, Verifikation und Anwendung von Windprofilerdaten in Österreich,* 133 Seiten, 29 Farbseiten, Wien 2004	25,00
33	414	Meteorologie	SPAN, N., A. FISCHER, M. KUHN, M. MASSIMO, M. BUTSCHEK:	*Radarmessungen der Eisdicke östereichischer Gletscher, Band I: Messungen 1995 bis 1998,* 154 Seiten, Wien 2005	25,00
34	415	Meteorologie	DOBESCH, H., D. NIKOLOV, L. MAKKONEN:	*Physical Processes, Modelling and Measuring of Icing Effects in Europe,* 75 Seiten, 18 Farbseiten, Wien 2005	25,00
35	416	Meteorologie	KAISER, A., E. PETZ, I. CUHALEV:	*Ermittlung der Gesamtbelastung durch Luftschadstoffe im Kurzzeitmittel anhand von Zeitreihen der Vor- und Zusatzbelastung; Vergleich mit statistischen Methoden Das zur Berechnung von Zeitreihen der Zusatzbelastung adaptierte ÖNORM M 9440 Modell ONGAUSSplus;* 61 Seiten, 6 Farbseiten, Wien 2005	25,00
36	417	Meteorologie	SVABIK, O., A. HOLZER:	*Kleinräumige, konvektiv verursachte Stürme und Wirbelstürme (Tornados) in Österreich*, 97 Seiten, 14 Farbseiten, Wien 2005	25,00
37	418	Meteorologie	WANG Y., T. HAIDEN, A. KANN:	*The operational Limited Area Modelling system at ZAMG: ALADIN-AUSTRIA*, 39 Seiten, 9 Farbseiten, Wien 2006	25,00